

Electronic Supplementary Information (ESI)

Genetically Encoded Fluorescent Unnatural Amino Acids and FRET Probes for Detecting Deubiquitinase Activities

Manjia Li,[†] Feifei Wang,[†] Long Yan,[†] Minghao Lu,[†] Yuqing Zhang,[†] and Tao Peng^{*, †, ‡}

[†] State Key Laboratory of Chemical Oncogenomics, Guangdong Provincial Key Laboratory of Chemical Genomics, School of Chemical Biology and Biotechnology, Peking University Shenzhen Graduate School, Shenzhen 518055, China

[‡] Institute of Chemical Biology, Shenzhen Bay Laboratory, Shenzhen 518132, China

* Correspondence: tpeng@pku.edu.cn

Table of Contents

<i>Supplementary figures</i>	4
Fig. S1	4
Fig. S2	5
Fig. S3	6
Fig. S4	7
Fig. S5	8
Fig. S6	9
Fig. S7	10
Fig. S8	11
Fig. S9	12
Fig. S10	13
Fig. S11	14
Fig. S12	15
Fig. S13	16
Fig. S14	17
Fig. S15	18
Fig. S16	19
Fig. S17	20
Fig. S18	21
Fig. S19	22
Fig. S20	23
Fig. S21	24
<i>Supplementary tables</i>	25
Table S1.	25
Table S2.	28
<i>Experimental procedures</i>	32
General methods and materials.....	32
Synthesis of the fluorescent unnatural amino acids ACouK and AFCouK	33
Plasmids and cloning.....	39

Screening of MmPylRS variants for ACouK and AFCouK incorporation	40
Incorporation of fluorescent unnatural amino acids into proteins in <i>E. coli</i>	40
Purification of proteins containing fluorescent unnatural amino acids from <i>E. coli</i>	41
Mass spectrometry analysis of purified proteins	41
Mammalian cell culture and transfection	41
Incorporation of fluorescent unnatural amino acids into proteins in mammalian cells	41
Photophysical characterization of fluorescent unnatural amino acids and proteins	42
Fluorescence imaging in live mammalian cells.....	42
Detection of deubiquitinase activities of USP7 and OTULIN by SDS-PAGE.....	43
Detection of deubiquitinase activities of USP7 and OTULIN by fluorescence.....	43
Screening of deubiquitinase inhibitors by FRET-based fluorescence detection	44
Western blotting	44
Quantification and statistical analysis	45
Protein sequences	45
<i>Reference</i>	47
<i>NMR spectra</i>	49
<i>Supplementary full gels and blots</i>	51

Supplementary figures

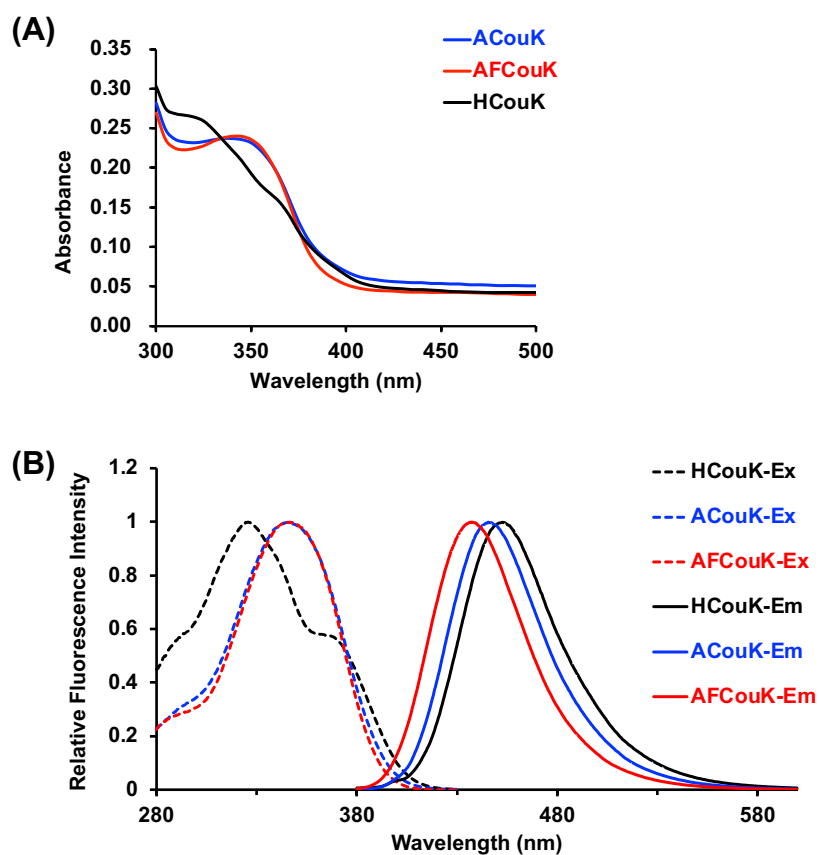


Fig. S1 (A) Absorption and (B) fluorescence spectra of fluorescent unnatural amino acids (UAAs). Coumarin-derived UAAs, i.e., ACouK, AFCouK, and HCouK were dissolved in PBS (20 mM, pH 7.4) at 10 μ M concentrations. Fluorescence excitation (Ex) and emission (Em) spectra were recorded with emission and excitation at 450 nm and 350 nm, respectively.

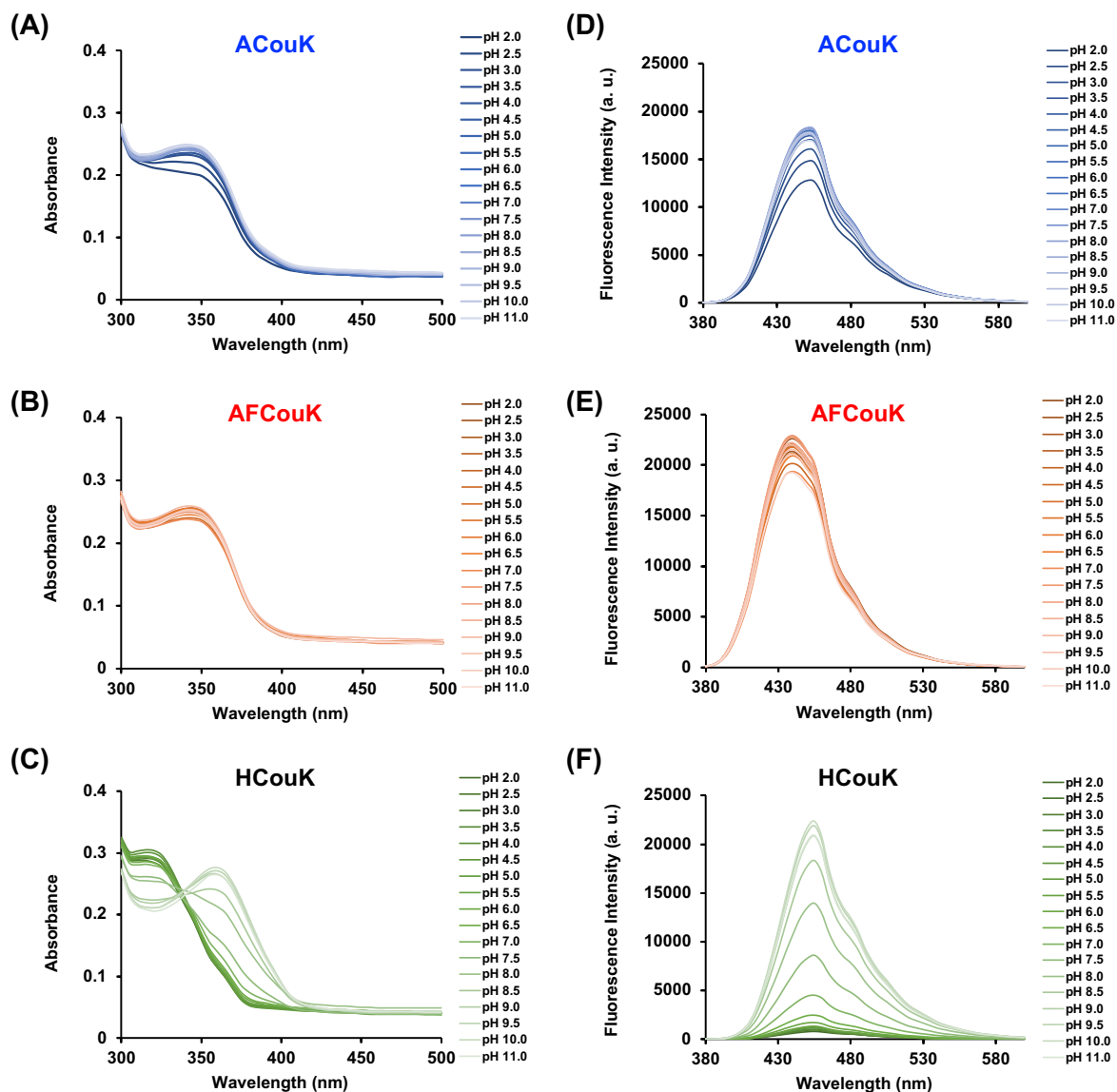


Fig. S2 Absorption (A–C) and fluorescence emission (D–F) spectra of ACouK (A, D), AFCouK (B, E), and HCOuK (C, F) under different pH conditions. ACouK, AFCouK, and HCOuK (10 μ M) were dissolved in aqueous buffers at varying pH values. Fluorescence emission spectra for ACouK and AFCouK were recorded with excitation at 350 nm. Fluorescence emission spectra for HCOuK were recorded with excitation at 330 nm.

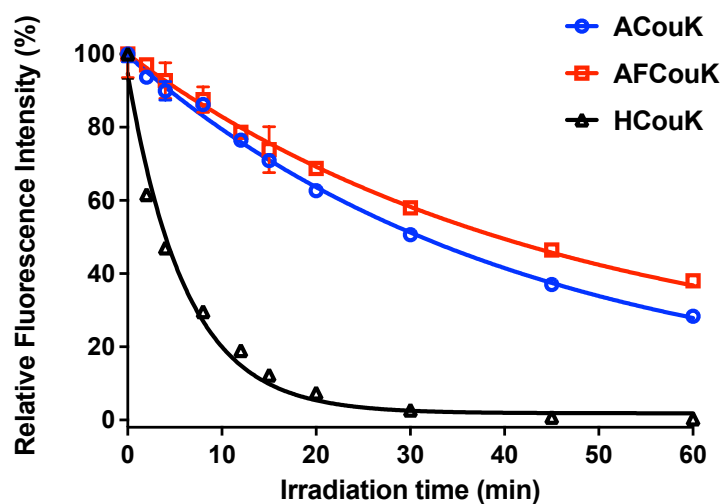


Fig. S3 Photostability of ACouK, AFCouK, and HCouK. ACouK, AFCouK, and HCouK were dissolved in PBS (20 mM, pH 7.4) and irradiated with 365 nm light for indicated time periods. The fluorescence intensities of ACouK, AFCouK, and HCouK at 450 nm, 440 nm, and 455 nm, respectively, were recorded with excitation at 350 nm, 350 nm, and 330 nm. Measurements were performed over three replicates and fits into exponential decays are shown as solid lines. Data are shown as mean \pm standard deviation ($n = 3$).

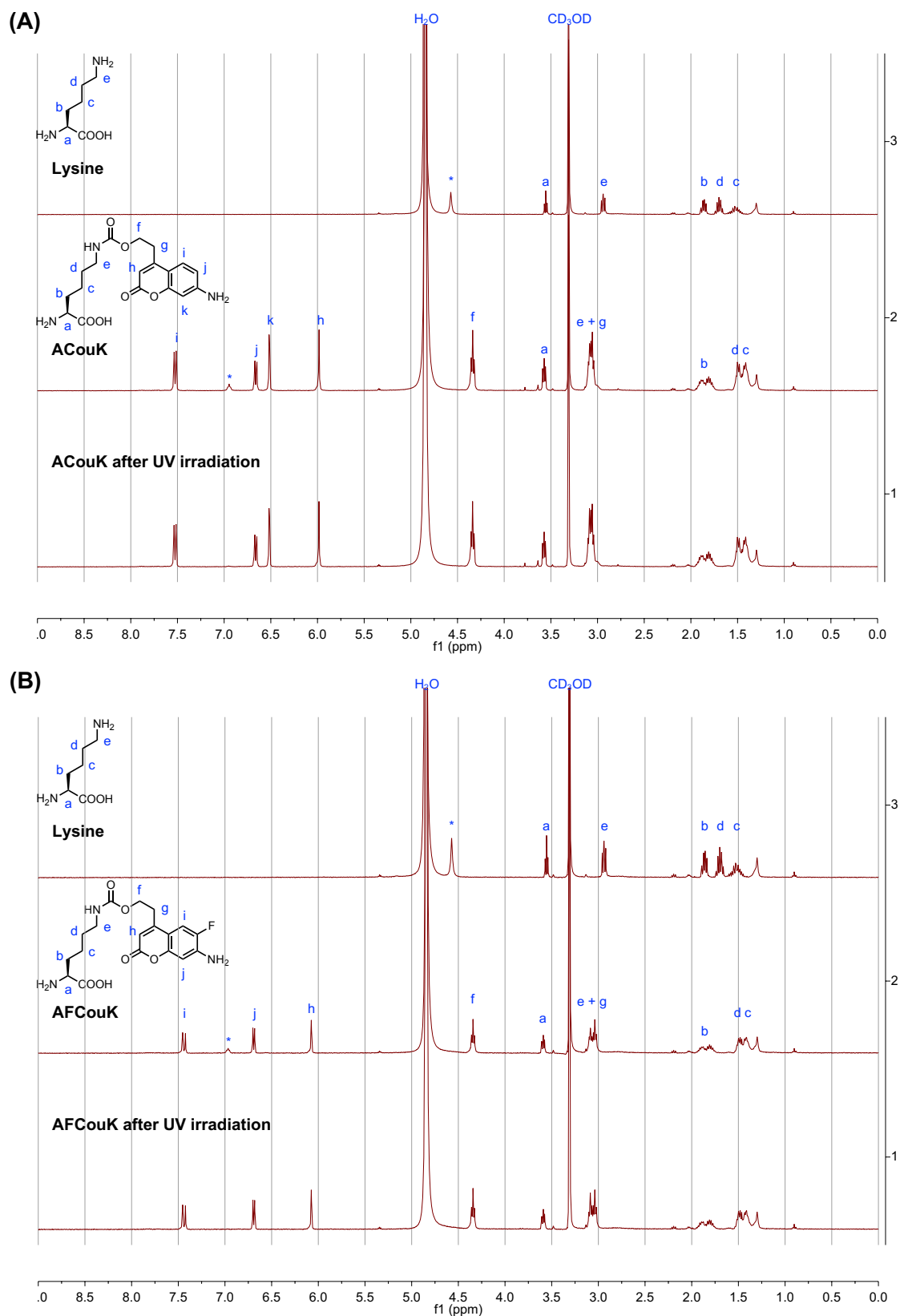


Fig. S4 Chemical stability of ACouK and AFCouK after continuous UV irradiation. (A) ^1H NMR of ACouK in CD_3OD before and after 365 nm UV irradiation for 30 min. (B) ^1H NMR of AFCouK in CD_3OD before and after 365 nm UV irradiation for 30 min. ^1H NMR spectra of free lysine are stacked for comparison. Asterisks show exchangeable protons.

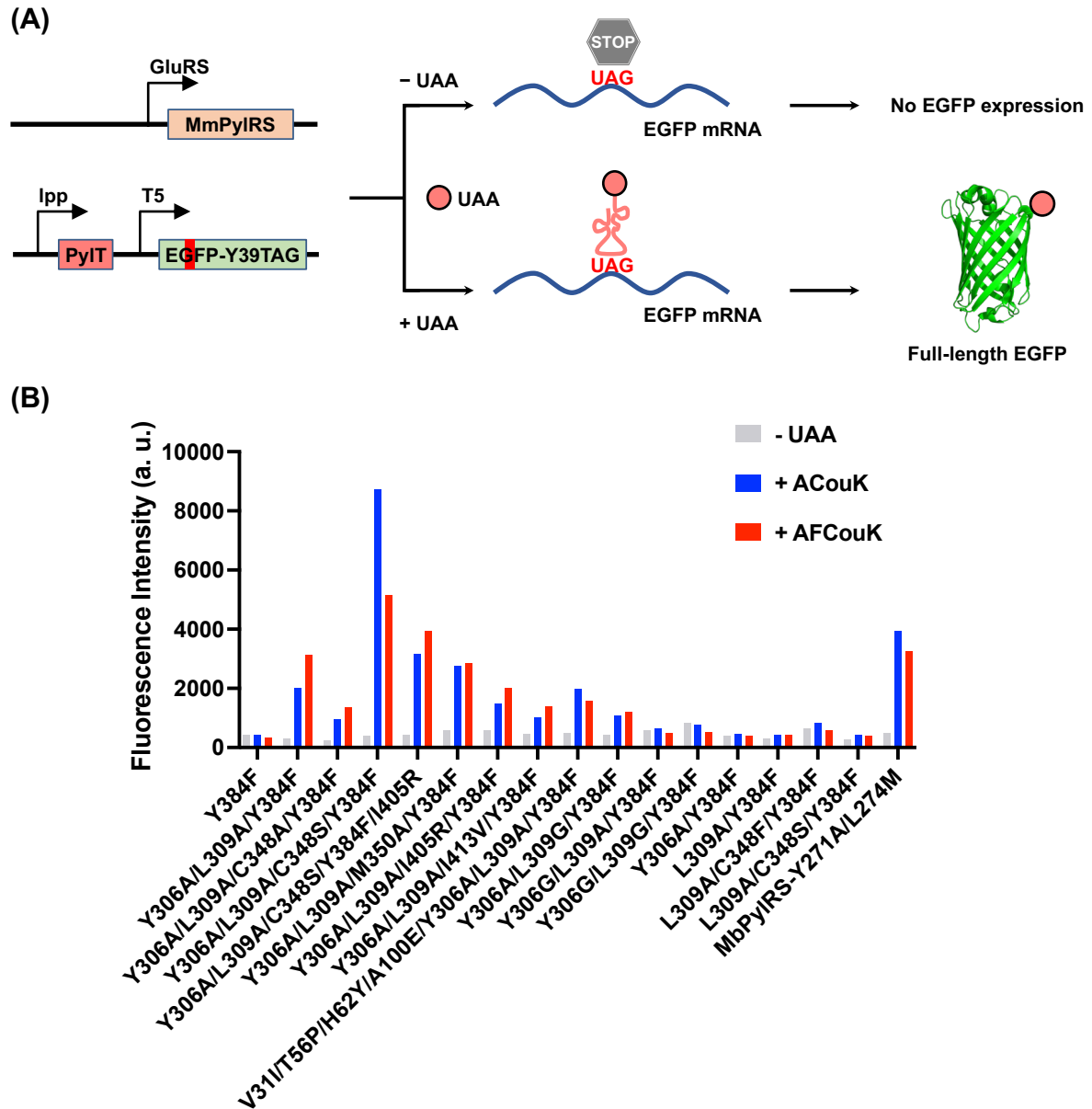


Fig. S5 (A) Schematic of the genetic code expansion technology for site-specific encoding of UAAs (e.g., ACouK and AFCouK) into proteins (e.g., EGFP-Y39TAG). (B) Screening of MmPylRS mutants for site-specific incorporation of ACouK and AFCouK into EGFP-Y39TAG in *E. coli*. The pLX-EGFP-Y39TAG plasmid was co-transformed with individual pBX-MmPylRS variant plasmid into *E. coli* strain BL21 (DE3). The transformed bacteria cells were grown in LB medium overnight at 37 °C and then inoculated by 1:100 dilution into LB medium. 1 mM ACouK or AFCouK was added into the bacterial culture when OD₆₀₀ reached 0.6. After 0.5 h incubation, protein expression was induced with 1 mM isopropyl-β-D-thiogalactoside (IPTG) for 10 h at 37 °C. The EGFP fluorescence intensity ($\lambda_{ex}/\lambda_{em} = 488/510$ nm) of individual bacterial culture was measured on a fluorescence microplate reader and compared with the control culture in the absence of UAA. The fluorescence was normalized to OD₆₀₀.

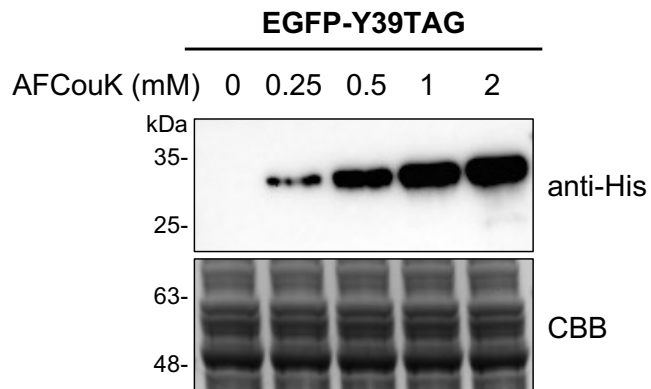


Fig. S6 Concentration-dependent incorporation of AFCouK into EGFP-Y39TAG in *E. coli*. The pLX-EGFP-Y39TAG-6*His plasmid was co-transformed with the pBX-ACouKRS plasmid into *E. coli* strain BL21 (DE3). The transformed bacteria cells were grown in LB medium overnight at 37 °C and then inoculated by 1:100 dilution into LB medium. AFCouK at different concentrations (from 0 to 2 mM) was added into the bacterial culture when OD₆₀₀ reached 0.6. After 0.5 h incubation, protein expression was induced with 1 mM IPTG for 10 h at 37 °C. Cells were harvested and lysed with 4% SDS lysis buffer. The resulting cell lysates were analyzed by western blotting and Coomassie Brilliant Blue (CBB) staining.

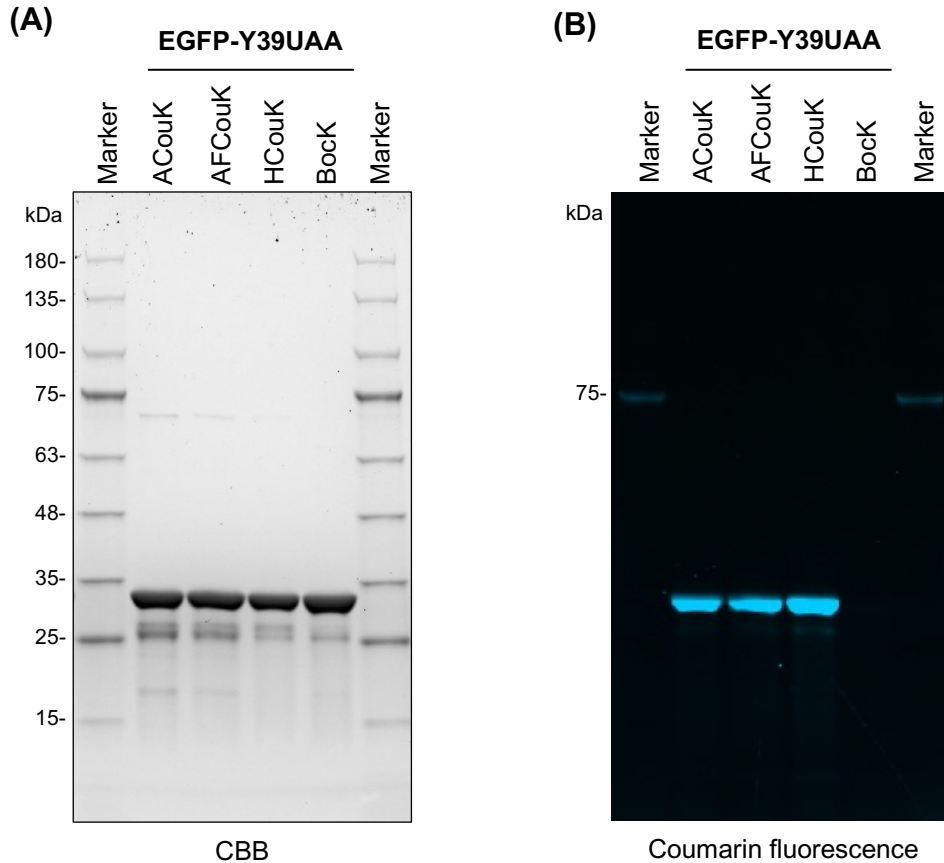


Fig. S7 Site-specific incorporation of coumarin-derived ACouK and AFCouK into EGFP-Y39TAG in *E. coli*. (A) SDS-PAGE gel analysis of purified EGFP-Y39UAA proteins containing coumarin-derived UAAs and BockK. (B) In-gel coumarin fluorescence analysis of purified EGFP-Y39UAA proteins containing coumarin-derived UAAs and BockK. The pLX-EGFP-Y39TAG plasmid was co-transformed with the appropriate PylRS plasmid into *E. coli* strain BL21 (DE3). The transformed bacteria cells were grown in LB medium overnight at 37 °C and then inoculated by 1:100 dilution into LB medium. ACouK, AFCouK, HCouK, or BockK (1 mM) was added into the bacterial culture when OD₆₀₀ reached 0.6. After 0.5 h incubation, protein expression was induced with 1 mM IPTG at 37 °C for 10 h. Cells were lysed with a sonic disruptor in Binding Buffer (20 mM Tris-HCl, 500 mM NaCl, 10% glycerol, 10 mM imidazole, pH 8.0) containing protease inhibitor cocktails, PMSF, deoxyribonuclease I, and lysozyme. The proteins were purified by Ni-NTA Sefinose Resin and analyzed by SDS-PAGE. In-gel coumarin fluorescence was performed on a Chemidoc MP imaging system with UV trans illumination as the excitation source.

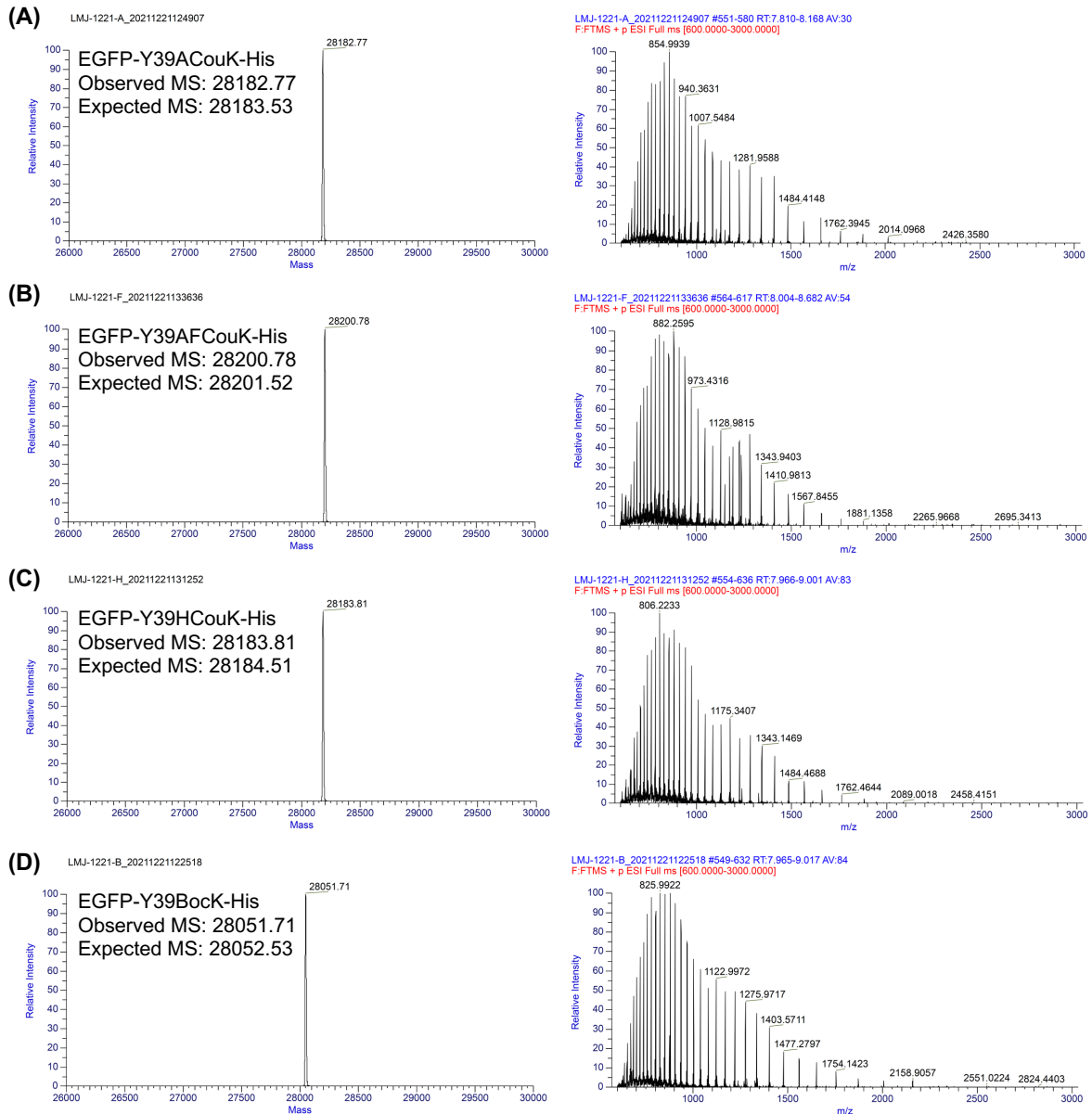


Fig. S8 Electrospray ionization mass spectrometry (ESI-MS) analyses of purified EGFP-Y39UAA proteins containing coumarin-derived UAAs and Bock. (A) Deconvoluted (left) and original (right) ESI-MS spectra of the His-tagged EGFP-Y39ACouK protein. Calculated mass of EGFP-Y39ACouK: 28183.53 Da; observed mass: 28182.77 Da. (B) Deconvoluted (left) and original (right) ESI-MS spectra of the His-tagged EGFP-Y39AFCouK protein. Calculated mass of EGFP-Y39AFCouK: 28201.52 Da; observed mass: 28200.78 Da. (C) Deconvoluted (left) and original (right) ESI-MS spectra of the His-tagged EGFP-Y39HCouK protein. Calculated mass of EGFP-Y39HCouK: 28184.51 Da; observed mass: 28183.81 Da. (D) Deconvoluted (left) and original (right) ESI-MS spectra of the His-tagged EGFP-Y39BocK protein. Calculated mass of EGFP-Y39BocK: 28052.53 Da; observed mass: 28051.71 Da. The pLX-EGFP-Y39TAG plasmid was co-transformed with the appropriate PylRS plasmid into *E. coli* strain BL21 (DE3). The transformed bacteria cells were grown in LB medium overnight at 37 °C and then inoculated by 1:100 dilution into LB medium. ACouK, AFCouK, HCouK, or Bock (1 mM) was added into the bacterial culture when OD₆₀₀ reached 0.6. After 0.5 h incubation, protein expression was induced with 1 mM IPTG at 37 °C for 10 h. Cells were lysed and the proteins were purified by Ni-NTA Sefinose Resin for ESI-MS analysis.

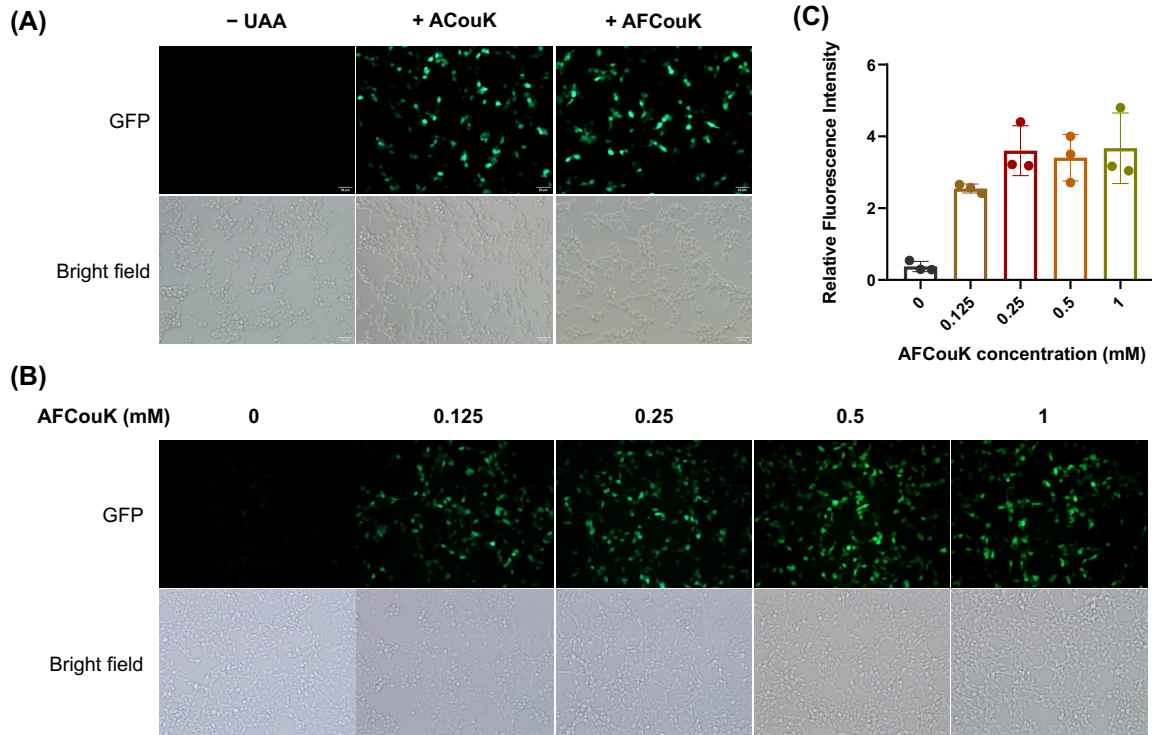


Fig. S9 Site-specific incorporation of ACouK and AFCouK into EGFP-Y39TAG in mammalian cells. (A) Fluorescence imaging of EGFP-Y39ACouK and EGFP-Y39AFCouK expression in HEK293T cells. (B) Fluorescence imaging of EGFP-Y39AFCouK expression in the presence of varying concentrations of AFCouK in HEK293T cells. Scale bars represent 50 μ m. (C) Quantification of fluorescence images shown in (B). Data are shown as mean \pm standard deviation ($n = 3$ independent experiments). HEK293T cells were transfected with plasmids of EGFP-Y39TAG and ACouKRS in the presence of ACouK or AFCouK (0.5 mM unless otherwise indicated) for 24 h and analyzed by fluorescence microscopy.

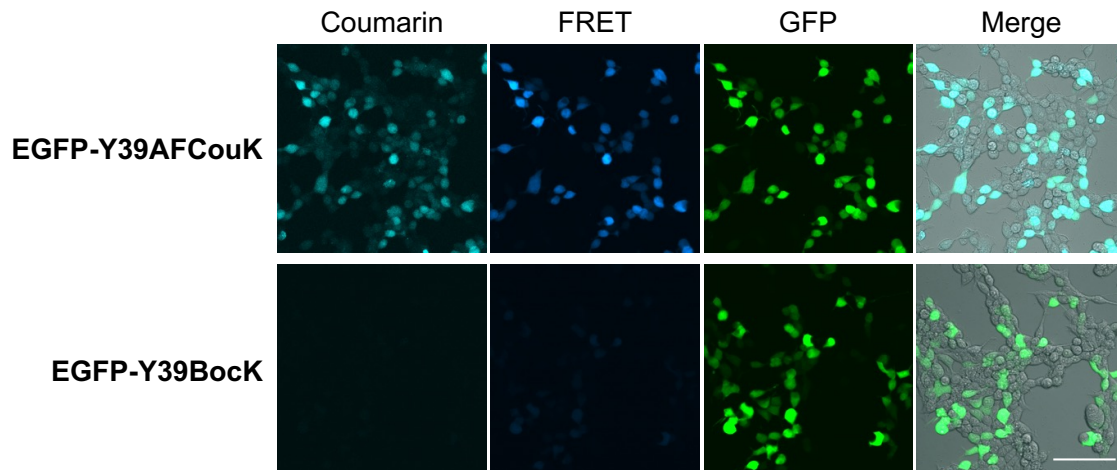


Fig. S10 Fluorescence imaging of FRET from AFCouK to EGFP in mammalian cells. HEK293T cells were transfected with plasmids of EGFP-Y39TAG and ACouKRS or MmPyIRS in the presence of AFCouK (0.5 mM) or BocK (0.1 mM), respectively, for 24 h and analyzed by confocal fluorescence microscopy. Scale bar represents 100 μ m. For the coumarin channel, the 405 nm laser was used as the excitation, and emission was collected between 410 nm to 480 nm. For the FRET channel, the 405 nm laser was used as the excitation, and emission was collected between 500 nm to 570 nm. For the EGFP channel, the 488 nm laser was used as the excitation, and emission was collected between 500 nm to 570 nm.

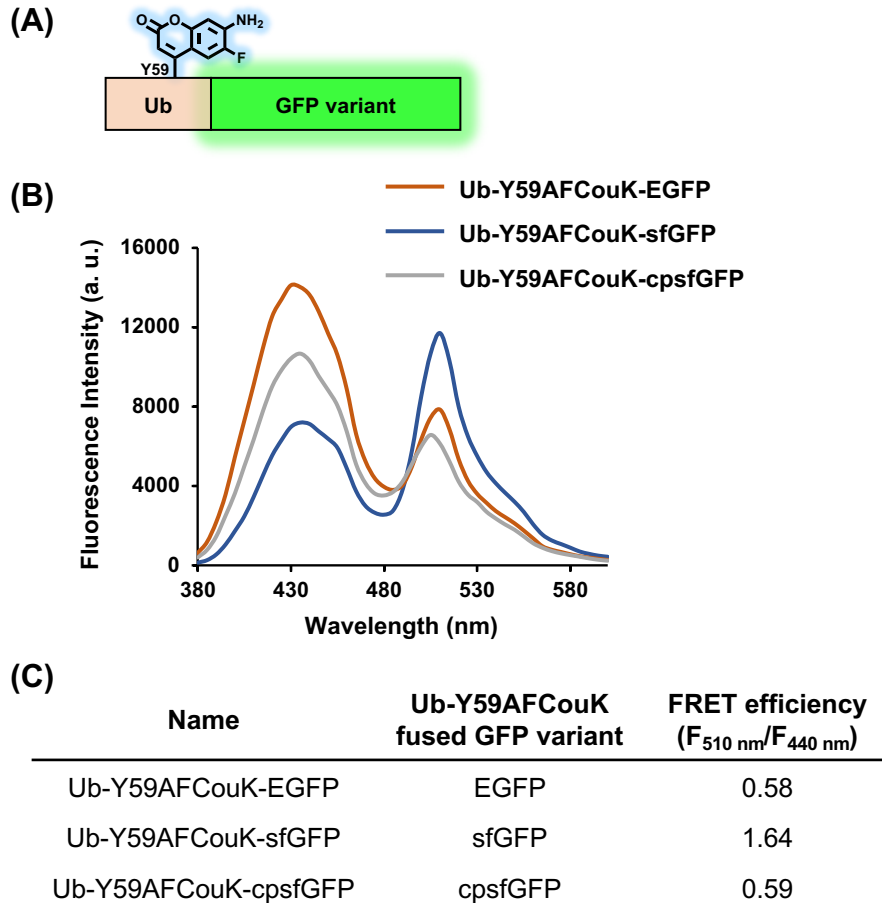


Fig. S11 Comparison of GFP variants as the FRET acceptors in Ub-Y59AFCouK fused GFP constructs. (A) Schematic of Ub-Y59AFCouK fused GFP variants examined in this study. (B) Fluorescence emission spectra of Ub-Y59AFCouK-sfGFP, Ub-Y59AFCouK-EGFP, and Ub-Y59AFCouK-cpsfGFP (0.5 μ M) in PBS (20 mM, pH 7.4) with excitation at 350 nm. (C) The FRET efficiency (measured as the ratio of GFP to AFCouK fluorescence at 510 nm and 440 nm, respectively), i.e., $F_{510 \text{ nm}}/F_{440 \text{ nm}}$, of Ub-Y59AFCouK-sfGFP, Ub-Y59AFCouK-EGFP, and Ub-Y59AFCouK-cpsfGFP shown in (B).

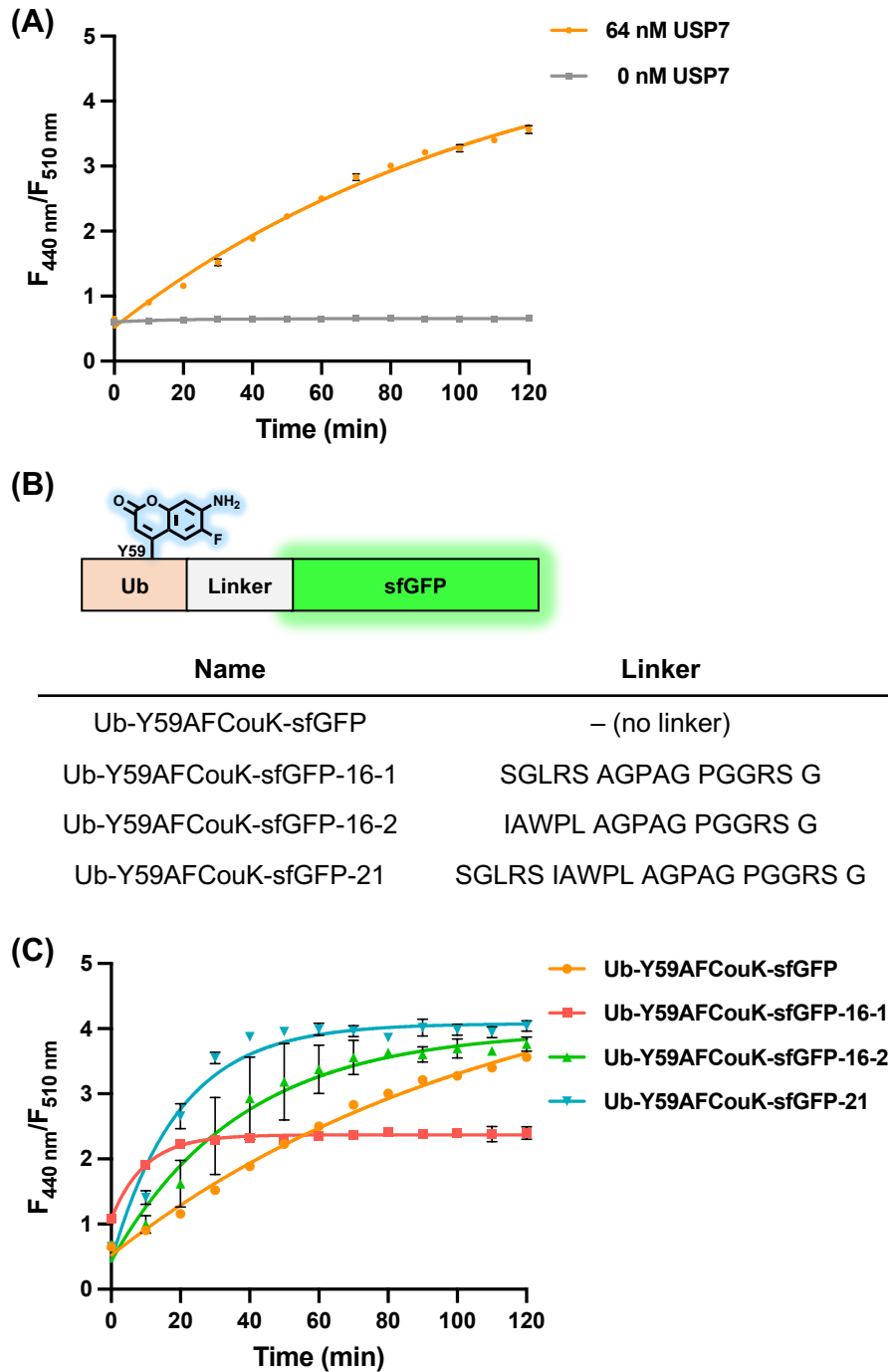


Fig. S12 Optimization of the linker length between Ub-Y59AFCouK and sfGFP in Ub-Y59AFCouK fused sfGFP constructs. (A) The fluorescence ratio of AFCouK to sfGFP at 440 nm and 510 nm, respectively, i.e., $F_{440 \text{ nm}}/F_{510 \text{ nm}}$, of Ub-Y59AFCouK-sfGFP increases with time in the presence of USP7 ($\lambda_{\text{ex}} = 350 \text{ nm}$). (B) The information of Ub-Y59AFCouK fused sfGFP constructs and linker sequences examined. (C) Fluorescence response kinetics of Ub-Y59AFCouK fused sfGFP constructs towards USP7. The purified Ub-Y59AFCouK fused sfGFP proteins ($0.5 \mu\text{M}$) were incubated with USP7 (64 nM) in DUB buffer ($100 \mu\text{L}$) at $37 \text{ }^\circ\text{C}$. Fluorescence intensities at 440 nm and 510 nm were measured with 350 nm excitation every 20 min over a period of 120 min. Data are shown as mean \pm standard deviation ($n = 3$).

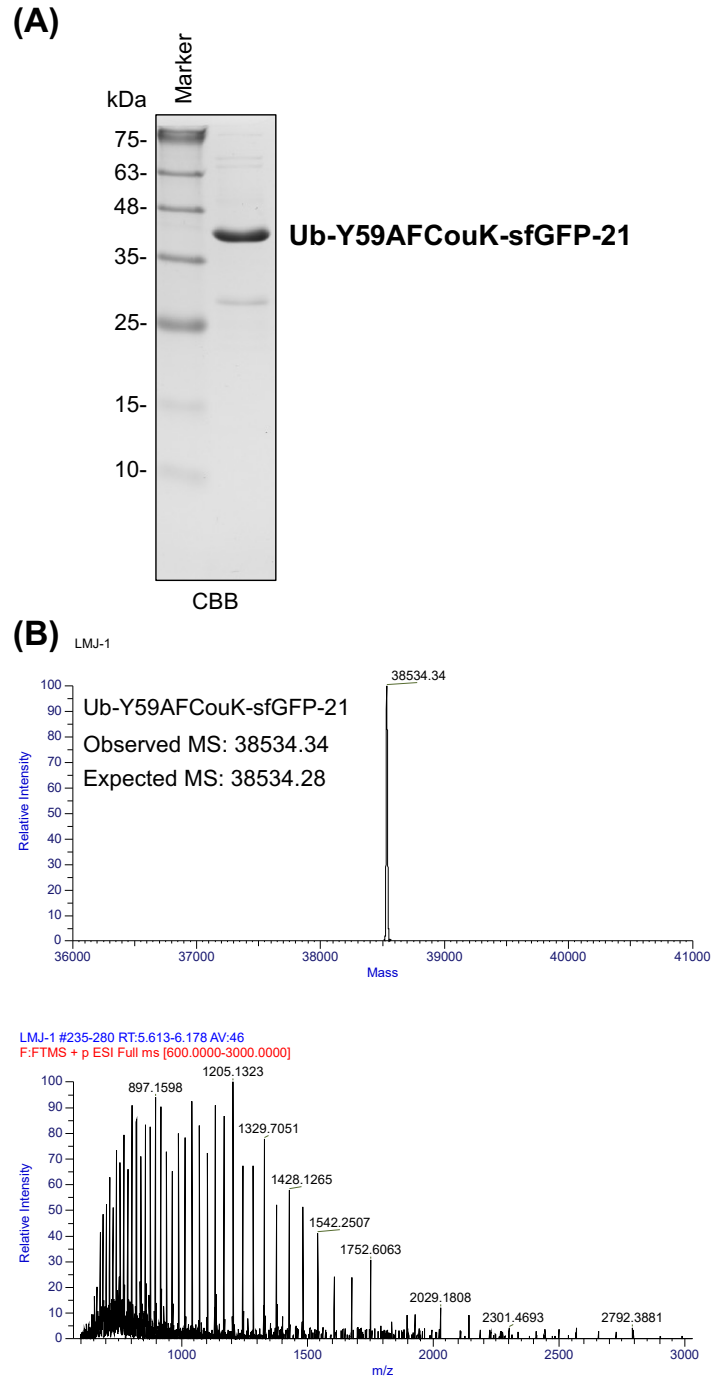


Fig. S13 Characterization of Ub-Y59AFCouK-sfGFP-21. (A) SDS-PAGE analysis of the purified Ub-Y59AFCouK-sfGFP-21 protein from *E. coli*. (B) ESI-MS analysis of the purified Ub-Y59AFCouK-sfGFP-21 protein. Calculated mass of Ub-Y59AFCouK-sfGFP-21: 38534.28 Da; observed mass: 38534.34 Da. Upper: the deconvoluted spectra; lower: the original ESI-MS spectra.

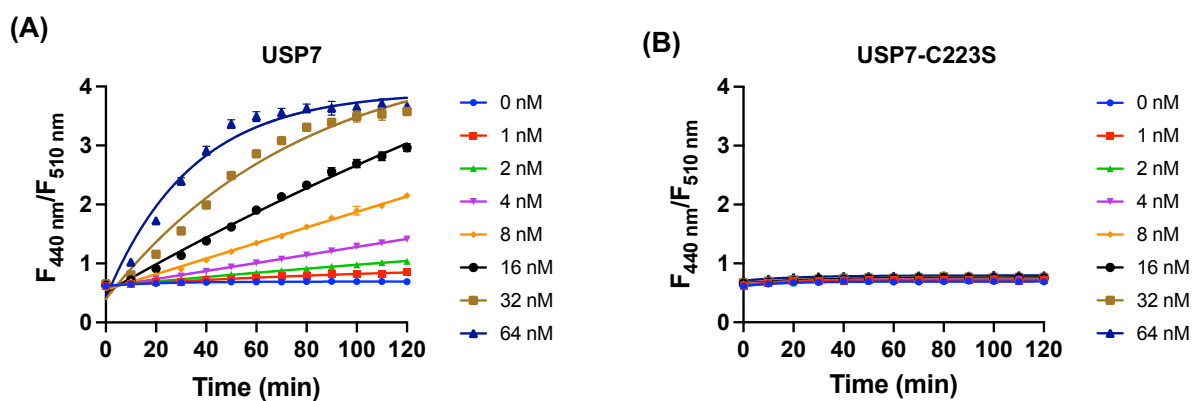


Fig. S14 Fluorescence detection of the deubiquitinase activity of USP7 using Ub-Y59AFCouK-sfGFP-21. (A) Fluorescence response kinetics of Ub-Y59AFCouK-sfGFP-21 towards USP7. (B) Fluorescence response kinetics of Ub-Y59AFCouK-sfGFP-21 towards USP7-C223S. The purified Ub-Y59AFCouK-sfGFP-21 protein (0.5 μM) was incubated with USP7 or USP7-C223S at varying concentrations (0–64 nM) in DUB buffer (100 μL) at 37 $^{\circ}\text{C}$. Fluorescence intensities at 440 nm and 510 nm were measured with 350 nm excitation every 20 min over a period of 120 min. Data are shown as mean \pm standard deviation ($n = 3$).

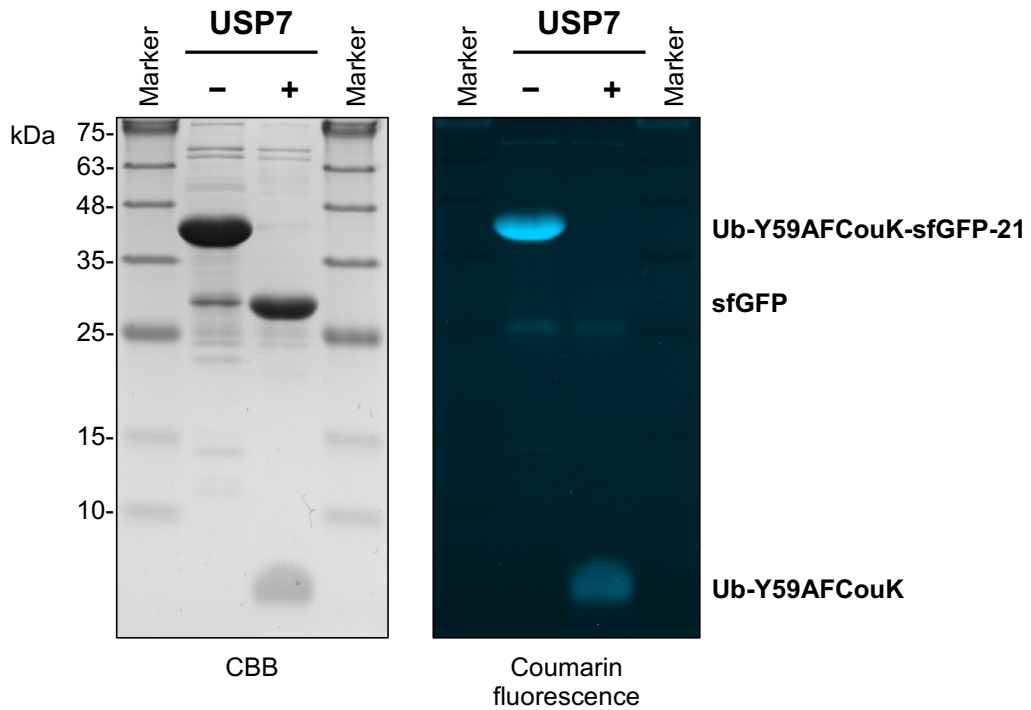


Fig. S15 SDS-PAGE analysis of the reaction between purified Ub-Y59AFCouK-sfGFP-21 and USP7. The purified Ub-Y59AFCouK-sfGFP-21 protein (10 μ M) was incubated with USP7 (50 nM) in DUB buffer at 37 $^{\circ}$ C for 6 h. Samples were resolved by SDS-PAGE, imaged by UV trans illumination for in-gel coumarin fluorescence analysis, and then stained with Coomassie Brilliant Blue (CBB). In-gel coumarin fluorescence was performed on a Chemidoc MP imaging system with UV trans illumination as the excitation source.

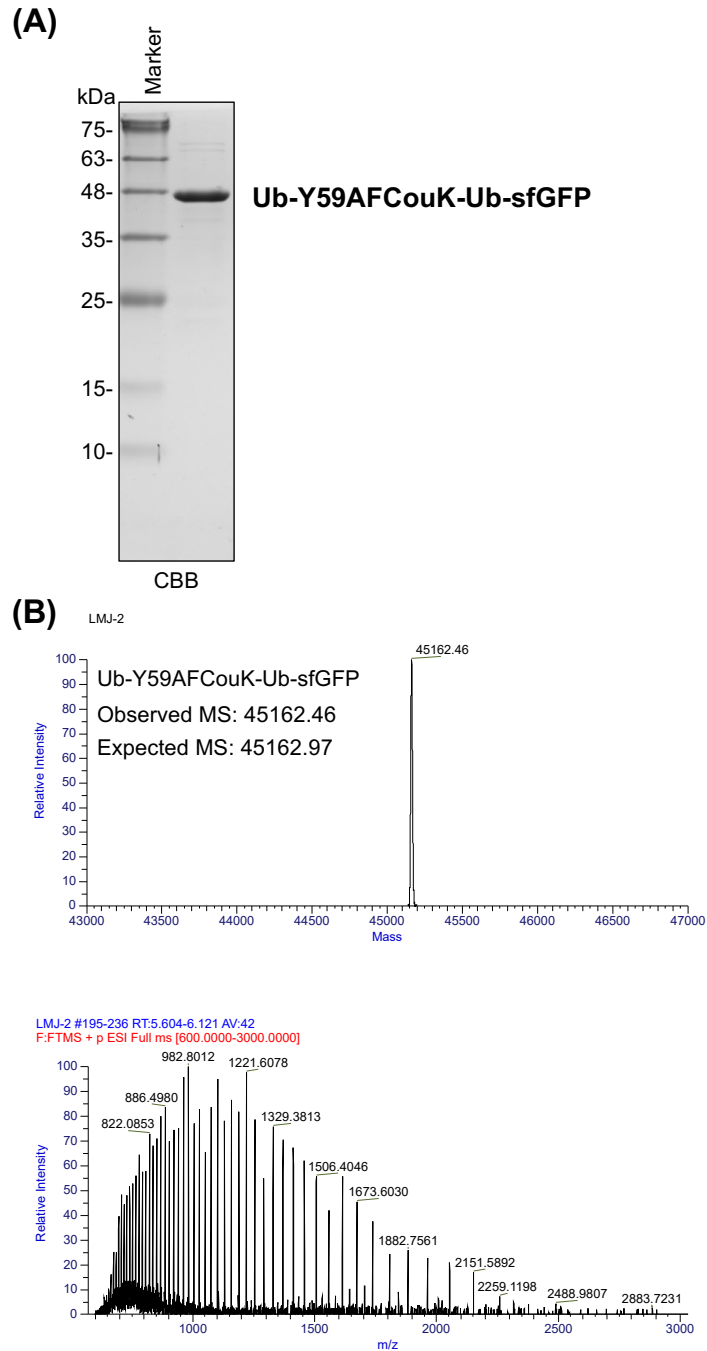


Fig. S16 Characterization of Ub-Y59AFCouK-Ub-sfGFP. (A) SDS-PAGE analysis of the purified Ub-Y59AFCouK-Ub-sfGFP protein from *E. coli*. (B) ESI-MS analysis of the purified Ub-Y59AFCouK-Ub-sfGFP protein. Calculated mass of Ub-Y59AFCouK-Ub-sfGFP: 45162.97 Da; observed mass: 45162.46 Da. Upper: the deconvoluted spectra; lower: the original ESI-MS spectra.

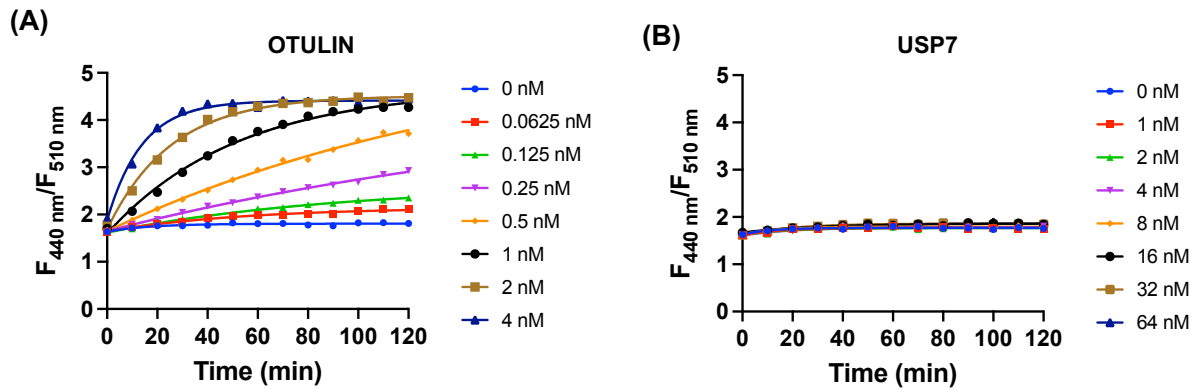


Fig. S17 Fluorescence detection of the deubiquitinase activity of OTULIN using Ub-Y59AFCouK-Ub-sfGFP. (A) Fluorescence response kinetics of Ub-Y59AFCouK-Ub-sfGFP towards OTULIN. (B) Fluorescence response kinetics of Ub-Y59AFCouK-Ub-sfGFP towards USP7. The purified Ub-Y59AFCouK-Ub-sfGFP protein (0.5 μ M) was incubated with OTULIN or USP7 at varying concentrations in DUB buffer (100 μ L) at 37 $^{\circ}$ C. Fluorescence intensities at 440 nm and 510 nm were measured with 350 nm excitation every 20 min over a period of 120 min. Data are shown as mean \pm standard deviation ($n = 3$).

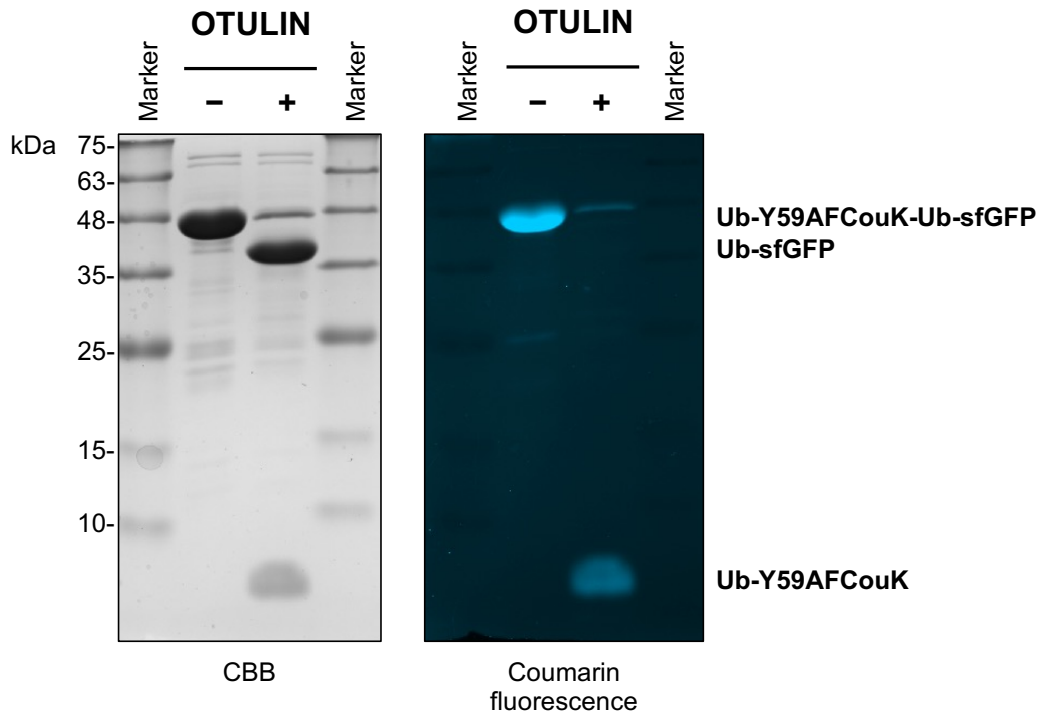


Fig. S18 SDS-PAGE analysis of the reaction between purified Ub-Y59AFCouK-Ub-sfGFP and OTULIN. The purified Ub-Y59AFCouK-Ub-sfGFP protein (10 μ M) was incubated with OTULIN (5 nM) in DUB buffer at 37 $^{\circ}$ C for 6 h. Samples were resolved by SDS-PAGE, imaged by UV trans illumination for in-gel coumarin fluorescence analysis, and then stained with Coomassie Brilliant Blue (CBB). In-gel coumarin fluorescence was performed on a Chemidoc MP imaging system with UV trans illumination as the excitation source.

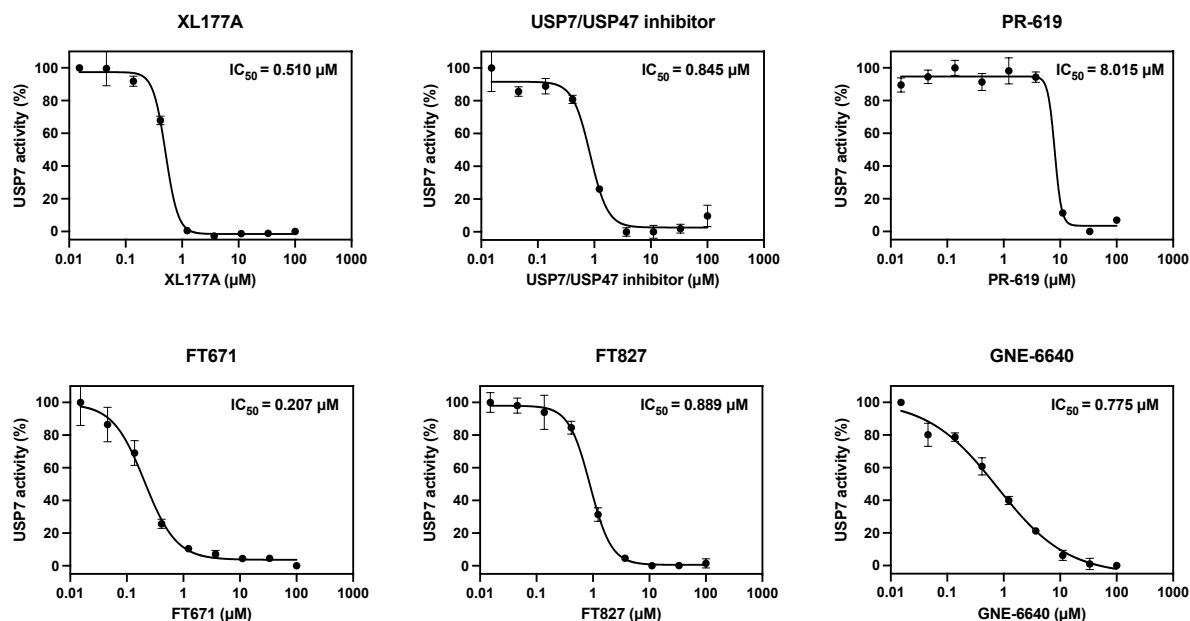


Fig. S19 IC_{50} analyses of selected known USP7 inhibitors. A subset of known USP7 inhibitors, including XL177A,¹ USP7/USP47 inhibitor,² PR-619,³ FT671,⁴ FT827,⁴ and GNE-6640,⁵ was identified in the screening and selected to validate the inhibition effects by determining their IC_{50} s for USP7. The compounds at varying concentrations were pre-incubated with USP7 (50 nM) in DUB buffer (20 μ L) at 37 °C for 30 min and then incubated with Ub-Y59AFCouK-sfGFP-21 (0.5 μ M) at 37 °C for 120 min. Fluorescence intensities at 440 nm and 510 nm were measured with 350 nm excitation and relative USP7 activities were calculated. Data are shown as mean \pm s. d. of triplicates ($n = 3$). IC_{50} s were calculated with a four-parameter “[inhibitor] vs. response - variable slope” model.

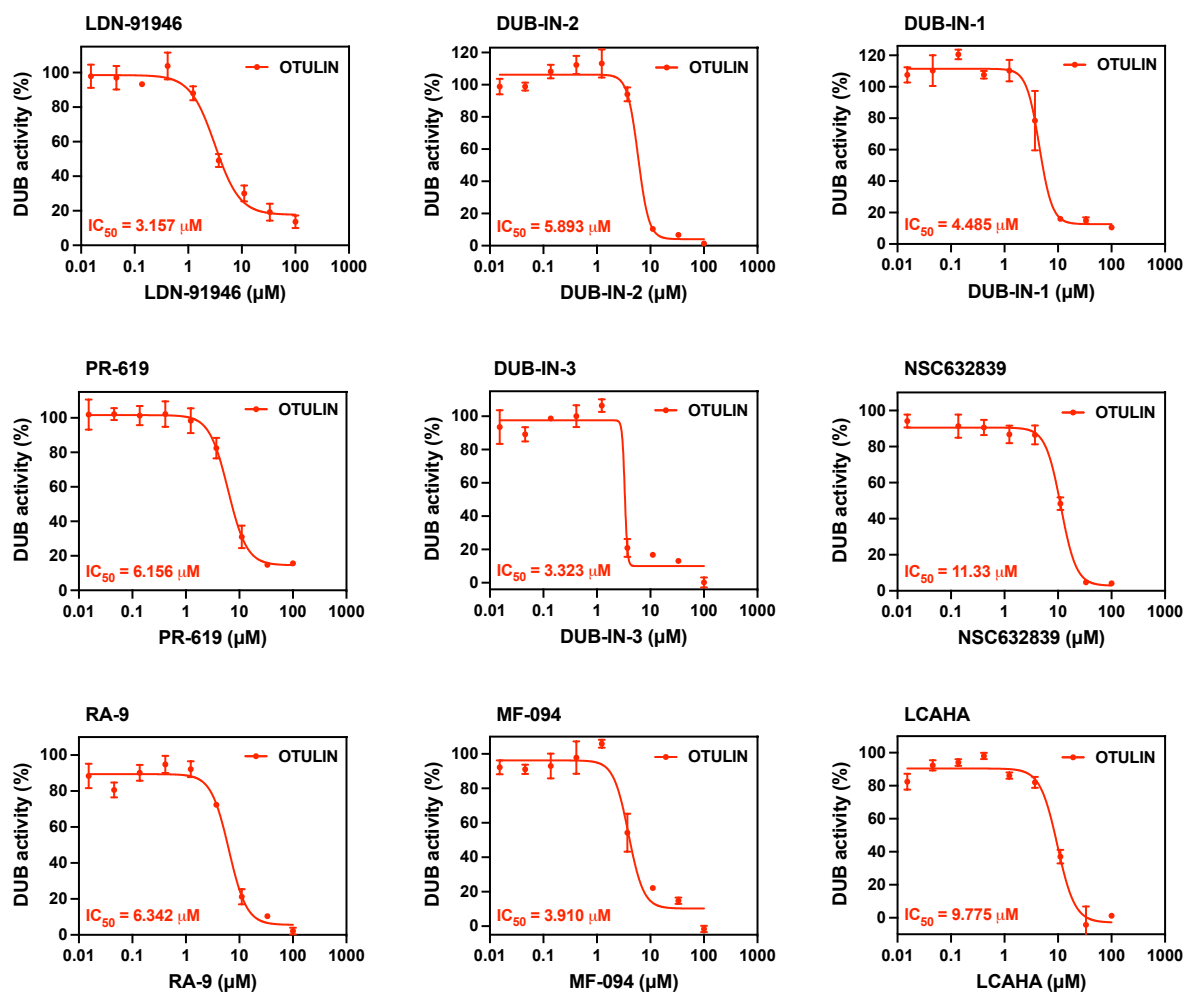


Fig. S20 IC₅₀ analyses of selected inhibitors for OTULIN. A subset of compounds was identified to be potential OTULIN inhibitors and selected to validate the inhibition effects by determining their IC₅₀s for OTULIN. The compounds at varying concentrations were pre-incubated with OTULIN (5 nM) in DUB buffer (20 μL) at 37 °C for 30 min and then incubated with Ub-Y59AFCouK-Ub-sfGFP (0.5 μM) at 37 °C for 120 min. Fluorescence intensities at 440 nm and 510 nm were measured with 350 nm excitation and OTULIN activities were calculated. Data are shown as mean ± s. d. of triplicates (*n* = 3). IC₅₀s were calculated with a four-parameter “[inhibitor] vs. response - variable slope” model.

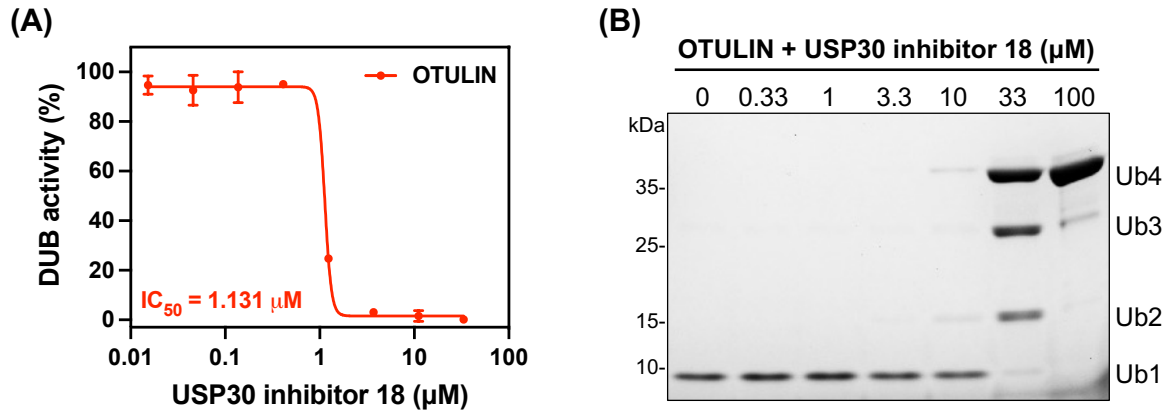
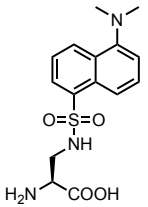
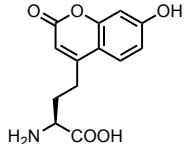
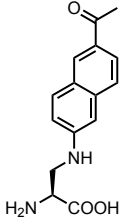
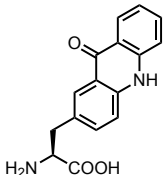
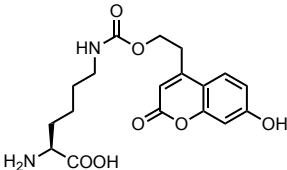
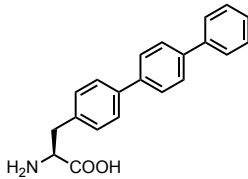


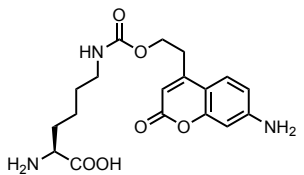
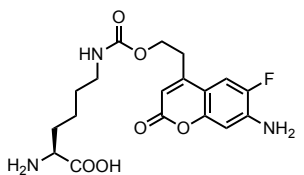
Fig. S21 Characterization of USP30 inhibitor 18 for inhibiting OTULIN. (A) IC_{50} analysis of USP30 inhibitor 18 for OTULIN. USP30 inhibitor 18 at varying concentrations was pre-incubated with OTULIN (5 nM) in DUB buffer (20 μ L) at 37 $^{\circ}$ C for 30 min and then incubated with Ub-Y59AFCouK-Ub-sfGFP (0.5 μ M) at 37 $^{\circ}$ C for 120 min. Fluorescence intensities at 440 nm and 510 nm were measured with 350 nm excitation and OTULIN activities were calculated. Data are shown as mean \pm s. d. of triplicates ($n = 3$). IC_{50} was calculated with a four-parameter “[inhibitor] vs. response - variable slope” model. (B) SDS-PAGE analysis of the inhibition effects of USP30 inhibitor 18 towards OTULIN. USP30 inhibitor 18 at varying concentrations was pre-incubated with OTULIN (5 nM) in DUB buffer at 37 $^{\circ}$ C for 30 min and then co-incubated with M1-linked tetra-ubiquitin (Ub4; 10 μ M) for 6 h. Samples were resolved by SDS-PAGE and stained with Coomassie Brilliant Blue. Ub4: tetra-ubiquitin; Ub3: tri-ubiquitin; Ub2: di-ubiquitin; Ub1: mono-ubiquitin.

Supplementary tables

Table S1. Summary of genetically encoded fluorescent UAAs.

UAA	λ_{ex} (nm)	λ_{em} (nm)	Φ_{F}	pH-dependence	RS/tRNA pair	Organism	Application	Year	Ref
 DanAla	340 (H ₂ O) ^a	550 (H ₂ O) ^a	0.10 (H ₂ O) ^a	n.d. ^b	<i>EcLeuRS</i>	<i>S. cerevisiae</i>	Protein unfolding	2006	[6]
 Hco	340 (H ₂ O) ^a	460 (H ₂ O) ^a	0.98 (H ₂ O) ^{a, c}	pH-sensitive (pK _a = ~7.8)	<i>MjTyrRS</i>	<i>E. coli</i>	Protein conformation change and localization	2006	[7]
 Anap	350 (H ₂ O) ^a	495 (H ₂ O) ^a	0.45 (H ₂ O) ^a	n.d. ^b	<i>EcLeuRS</i>	<i>S. cerevisiae</i> , mammalian cells	Protein structural change, dynamics, and localization; FRET probes	2009, 2013	[8-9]

UAA	λ_{ex} (nm)	λ_{em} (nm)	Φ_{F}	pH-dependence	RS/tRNA pair	Organism	Application	Year	Ref
 <p>Acid</p>	386 (H ₂ O) ^a	420 (H ₂ O) ^a	0.93 (H ₂ O) ^a	n.d. ^b	MjTyrRS, MbPylRS	<i>E. coli</i> , mammalian cells	Fluorescence lifetime and FRET study	2013, 2021	[10- 11]
 <p>HCouK</p>	330 (PBS) ^d	455 (PBS) ^d	0.62 (PBS) ^d	pH-sensitive (pK _a = 7.76)	MbPylRS	<i>E. coli</i> , mammalian cells	Protein localization	2014	[12]
 <p>Terphenyl UAA</p>	280 (CHCl ₃) ^e	342 (CHCl ₃) ^e	0.49 (CHCl ₃) ^e	n.d. ^b	MjTyrRS	<i>E. coli</i>	Modulation of GFP fluorescence	2015	[13]

UAA	λ_{ex} (nm)	λ_{em} (nm)	Φ_{F}	pH-dependence	RS/tRNA pair	Organism	Application	Year	Ref
 ACouK	360 (PBS) ^d	450 (PBS) ^d	0.80 (PBS) ^d	pH-insensitive	<i>MmPylRS</i>	<i>E. coli</i> , mammalian cells	FRET probes	2022	This work
 AFCouK	360 (PBS) ^d	440 (PBS) ^d	0.98 (PBS) ^d	pH-insensitive	<i>MmPylRS</i>	<i>E. coli</i> , mammalian cells	FRET probes, DUB detection	2022	This work

^a Data measured in H₂O.¹¹

^b Not determined.

^c Data of the anionic form measured in H₂O.¹¹

^d Data measured in PBS (pH = 7.4) and acquired in this study.

^e Data for *p*-terphenyl.¹⁴

Table S2. Summary of inhibitors screened in this study.^a

No.	Product Name	CAS No.	Plate Location	Cat. No. ^b	Information	USP7 inhibition (%) ^c		OTULIN inhibition (%) ^c	
						1 μ M	10 μ M	1 μ M	10 μ M
1	USP7-IN-8	2009273-60-1	A2	HY-134817	A selective USP7 inhibitor (IC ₅₀ = 1.4 μ M).	18.03	78.58	-0.74	43.06
2	N-ethylmaleimide (NEM)	128-53-0	A3	HY-D0843	A cysteine protease inhibitor and a deubiquitinating enzyme inhibitor.	7.25	-3.12	14.58	31.21
3	USP30 inhibitor 18	2242582-40-5	A4	HY-141659	A selective USP30 inhibitor (IC ₅₀ = 0.02 μ M).	1.54	14.22	30.11	90.7
4	STD1T	893075-58-6	A5	HY-124855	A deubiquitinase USP2a inhibitor (IC ₅₀ = 3.3 μ M).	2.54	7.12	18.01	20.82
5	LCAHA	117094-40-3	A6	HY-120458	A USP2a inhibitor (IC ₅₀ = 9.7 μ M).	-0.16	-2.07	26.66	70.61
6	6RK73	1895050-66-4	A7	HY-133118	A covalent irreversible and specific UCHL1 inhibitor (IC ₅₀ = 0.23 μ M).	6.21	-0.23	18.8	24.32
7	LDN-91946	439946-22-2	A8	HY-12989	A potent, selective and uncompetitive UCH-L1 inhibitor (K _{i app} = 2.8 μ M).	-3.38	-10.8	21.94	36.12
8	FT206	2278274-34-1	A9	HY-138698	An inhibitor of carboxamides as ubiquitin-specific protease.	6.46	16.79	21.27	69.61
9	XL177A	2417089-74-6	A10	HY-138794	A highly potent and selective irreversible USP7 inhibitor (IC ₅₀ = 0.34 nM).	86.78	89.17	-3.7	-1.99
10	USP25/28 inhibitor AZ1	2165322-94-9	A11	HY-117370	An orally active, selective, noncompetitive, dual USP25/28 inhibitor (IC ₅₀ = 0.7 and 0.6 μ M).	-11.06	-0.82	16.67	38.39

No.	Product Name	CAS No.	Plate Location	Cat. No. ^b	Information	USP7 inhibition (%) ^c		OTULIN inhibition (%) ^c	
						1 μ M	10 μ M	1 μ M	10 μ M
11	ML-323	1572414-83-5	B2	HY-17543	A reversible and potent USP1-UAF1 inhibitor (IC ₅₀ = 76 nM).	3.77	-7.68	14.6	40.87
12	IU1	314245-33-5	B3	HY-13817	A special USP14 inhibitor (IC ₅₀ = 4-5 μ M).	0.9	-6.48	11.67	27.31
13	USP7/USP47 inhibitor	1247825-37-1	B4	HY-13487	A selective USP7/USP47 inhibitor (EC ₅₀ = 0.42 and 1.0 μ M).	89.13	85.53	11.74	99.81
14	USP7-IN-1	1381291-36-6	B5	HY-16709	A selective and reversible inhibitor of USP7 (IC ₅₀ = 77 μ M).	2.38	3.4	-3.46	33.24
15	HBX 19818	1426944-49-1	B6	HY-17540	A specific inhibitor of USP7 (IC ₅₀ = 28.1 μ M).	1.67	14.82	23.28	43.41
16	DUB-IN-2	924296-19-5	B7	HY-50737A	A potent deubiquitinase inhibitor (IC ₅₀ = 0.28 μ M).	7.5	-4.88	7.94	78.31
17	TCID	30675-13-9	B8	HY-18638	A potent and selective UCH-L3 inhibitor (IC ₅₀ = 0.6 μ M).	3.12	18.76	85.7	101.79
18	DUB-IN-1	924296-18-4	B9	HY-50736	An active USP8 inhibitor (IC ₅₀ = 0.85 μ M).	3.34	12.03	0.13	73.71
19	LDN-57444	668467-91-2	B10	HY-18637	A reversible, competitive and site-directed inhibitor of UCH-L1 (IC ₅₀ = 0.88 μ M, K _i = 0.40 μ M).	6.96	-9.75	11.87	40.82
20	IU1-47	670270-31-2	B11	HY-122243	A potent and specific USP14 inhibitor (IC ₅₀ = 0.6 μ M).	-0.45	13.81	16.51	37.38
21	SJB3-019A	2070015-29-9	C2	HY-80012	A potent and novel USP1 inhibitor (IC ₅₀ = 0.0781 μ M).	-3.19	9.79	9.39	12.15

No.	Product Name	CAS No.	Plate Location	Cat. No. ^b	Information	USP7 inhibition (%) ^c		OTULIN inhibition (%) ^c	
						1 μ M	10 μ M	1 μ M	10 μ M
22	Degrasyn	856243-80-6	C3	HY-13264	A cell-permeable DUB inhibitor, directly inhibiting USP9x, USP5, USP14, and UCH37.	9.31	7.5	34.76	41.13
23	PR-619	2645-32-1	C4	HY-13814	A broad-range and reversible DUB inhibitor (EC_{50} = 3.93, 4.9, 6.86, 7.2, and 8.61 μ M for USP4, USP8, USP7, USP2, and USP5, respectively).	11.25	91.89	25.6	67.13
24	GSK2643943A	2449301-27-1	C5	HY-111458	A DUB inhibitor (IC_{50} = 160 nM for USP20).	29.81	63.59	67.66	91.56
25	DUB-IN-3	924296-17-3	C6	HY-50737	A potent USP inhibitor (IC_{50} = 0.56 μ M for USP8).	-4.62	-5.89	6.65	73.59
26	ML364	1991986-30-1	C7	HY-100900	A selective USP2 inhibitor (IC_{50} = 1.1 μ M).	-2.4	87.81	27.86	70.42
27	MF-094	2241025-68-1	C8	HY-112438	A potent and selective USP30 inhibitor (IC_{50} = 120 nM).	-1.89	5	28.31	79.07
28	EOAI3402143	1699750-95-2	C9	HY-111408	A DUB inhibitor for Usp9x/Usp24 and Usp5.	5.65	16.14	5.68	12.32
29	6-Thioguanine	154-42-7	C10	HY-13765	An inhibitor of SARS and MERS coronavirus PLpros and USP2 (IC_{50} = 25 and 40 μ M for PLpros and USP2, respectively).	-4.68	-10.54	2.36	6.5
30	SJB2-043	63388-44-3	C11	HY-15757	An inhibitor of the native USP1/UAF1 complex (IC_{50} = 544 nM).	-2.63	-7.92	10.4	15.56
31	P005091	882257-11-6	D2	HY-15667	A selective and potent inhibitor of USP7 (EC_{50} = 4.2 μ M).	0.88	39.29	4.52	1.74

No.	Product Name	CAS No.	Plate Location	Cat. No. ^b	Information	USP7 inhibition (%) ^c		OTULIN inhibition (%) ^c	
						1 μ M	10 μ M	1 μ M	10 μ M
32	NSC632839	157654-67-6	D3	HY-100708	A nonselective inhibitor for USP2, USP7, and SENP2 (EC ₅₀ = 45, 37, and 9.8 μ M, respectively).	-5.33	-9.88	20.85	87.71
33	P 22077	1247819-59-5	D4	HY-13865	A cell-permeable USP7 inhibitor (EC ₅₀ = 8.01 μ M).	12.61	38.81	9.52	7.27
34	FT671	1959551-26-8	D5	HY-107985	A potent, non-covalent and selective USP7 inhibitor (IC ₅₀ = 52 nM).	76.6	93.23	2.44	8.44
35	GNE-6776	2009273-71-4	D6	HY-107986	A selective and orally bioavailable USP7 inhibitor.	5.95	83.72	7.37	4.39
36	GRL0617	1093070-16-6	D7	HY-117043	A potent, selective and competitive noncovalent inhibitor of SARS-CoV PLpro (IC ₅₀ = 0.6 μ M).	-0.29	4.77	6.05	3.14
37	FT827	1959537-86-0	D8	HY-111350	A selective and covalent USP7 inhibitor (K _i = 4.2 μ M).	22.93	95.69	17.74	21.17
38	GNE-6640	2009273-67-8	D9	HY-112937	A selective and non-covalent inhibitor of USP7 (IC ₅₀ = 0.75 μ M).	33.95	88.78	0.75	4.32
39	BAY 11-7082	19542-67-7	D10	HY-13453	An inhibitor of USP7 and USP21 (IC ₅₀ = 0.19 and 0.96 μ M, respectively).	20.24	17.45	5.7	9.67
40	RA-9	919091-63-7	D11	HY-136528	A potent and selective inhibitor for proteasome-associated DUBs.	12	16.15	20.88	85.99

^a The inhibitors were purchased from MedChemExpress.

^b Shown are the catalog numbers of MedChemExpress.

^c Shown are the mean inhibition rates from three replicates ($n = 3$).

Experimental procedures

General methods and materials

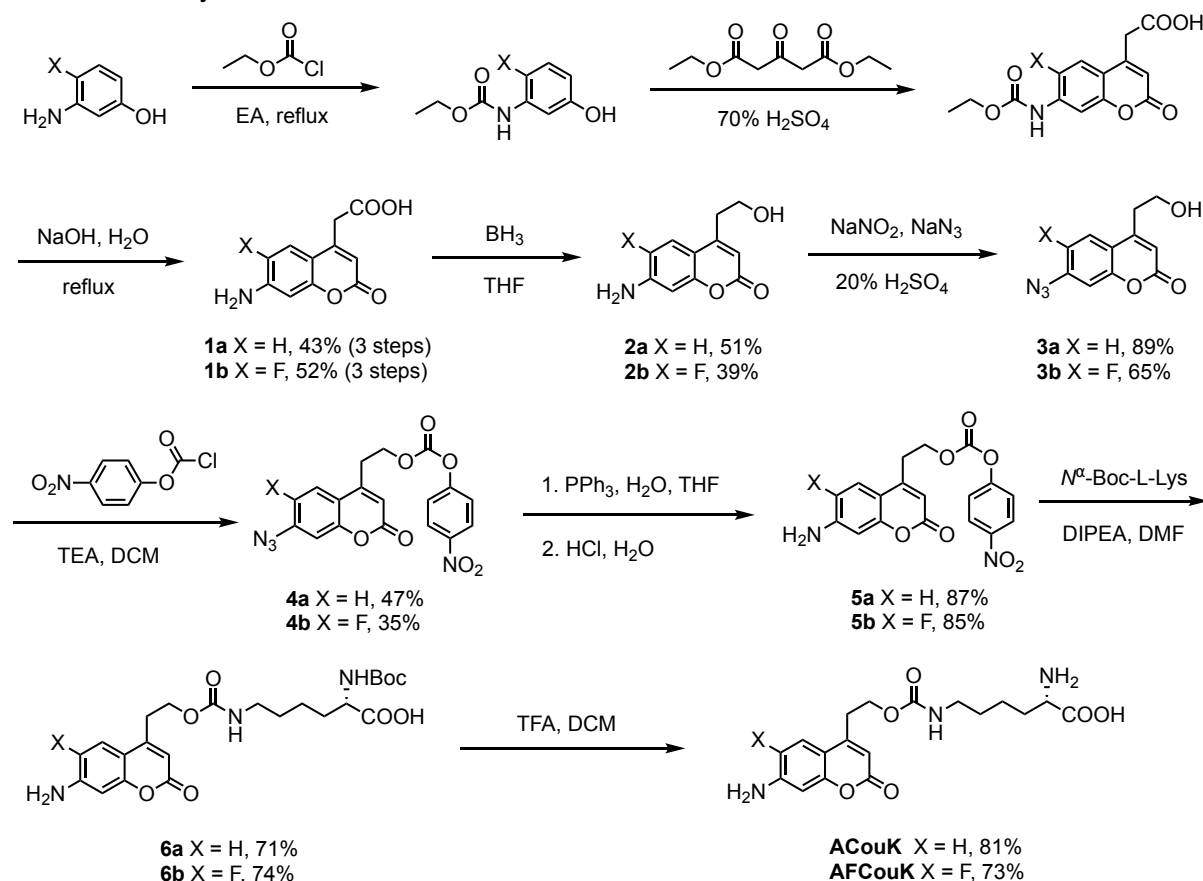
Chemicals and solvents for organic synthesis were obtained from commercial sources and used directly as received without further purification, unless otherwise noted. Chemical reactions were performed in oven-dried round-bottom flasks and monitored by TLC on silica gel 60 GF254 glass plates (Qingdao Haiyang Chemical Co., Ltd). Spots on TLC were visualized by UV irradiation (254 nm) and staining with potassium permanganate (KMnO₄) or phosphomolybdic acid (PMA). Flash column chromatography was conducted with silica gel (200-300 mesh, reagent grade) from Accela ChemBio Co., Ltd. Nuclear magnetic resonance (NMR) spectra were recorded in CDCl₃, CD₃OD, or (CD₃)₂SO at room temperature on Bruker Avance NMR Spectrometers operating at 300, 400, or 500 MHz for proton. Chemical shifts (δ) are reported in ppm, and coupling constants (*J* values) are reported in Hz. ¹H NMR chemical shifts are calibrated using tetramethylsilane (TMS, δ = 0.00 ppm) in CDCl₃ as the internal standard or with the residual solvent peaks of CD₃OD (δ = 3.31 ppm) or (CD₃)₂SO (δ = 2.50 ppm). ¹³C NMR chemical shifts are calibrated with the residual solvent peaks of CDCl₃ (δ = 77.16 ppm), CD₃OD (δ = 49.00 ppm), or (CD₃)₂SO (δ = 39.52 ppm). High resolution mass spectra (HRMS) were recorded on a Q Exactive Focus (Thermo Fisher Scientific) mass spectrometer using the ESI source.

PfuUltra High-Fidelity DNA Polymerase was obtained from Agilent Technologies for PCR amplification reactions. Restriction enzymes and dNTPs were obtained from New England Biolabs. Oligonucleotide primers and gene fragments were synthesized by Genewiz or Tsingke Biotechnology. Site-directed mutagenesis was performed with QuikChange II Site-Directed Mutagenesis Kit (Agilent Technologies) with primers designed by Agilent Primer Design Program. Gibson assembly was carried out with Seamless Cloning Kit (Beyotime). Plasmid DNA isolation was carried out with Plasmid Mini/Midi Kit (Omega). Polyethylenimine (PEI) was purchased from Polysciences. Protease inhibitor cocktail (cOmplete ULTRA mini Tablets) was purchased from Roche. Isopropyl- β -D-thiogalactoside (IPTG), kanamycin, and chloramphenicol were purchased from Sangon Biotech. *N*^ε-Boc-L-Lysine (Bock) was purchased from Adamas and dissolved in 0.1 M NaOH as the stock solution (2 M). Coumarin-derived fluorescent unnatural amino acids were dissolved in DMSO as the stock solution (500 mM). Optical density (OD) was measured with a UV-Vis spectrophotometer (Techcomp UV-1000). Absorption spectra and fluorescence spectra were recorded on a Biotek Synergy H1 microplate reader. Confocal fluorescence imaging was performed with a Nikon A1R confocal fluorescence microscope. In-gel fluorescence and Western blotting analyses were recorded on a Chemidoc MP imaging system (Biorad).

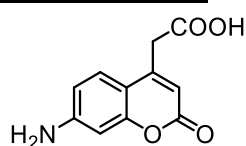
Synthesis of the fluorescent unnatural amino acids ACouK and AFCouK

The fluorescent unnatural amino acid **HCouK** was synthesized according to the literature.¹² **ACouK** and **AFCouK** were synthesized as shown in Scheme S1.

Scheme S1. Synthetic scheme of ACouK and AFCouK



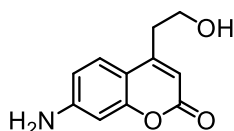
Synthesis of ACouK



2-(7-amino-2-oxo-2H-chromen-4-yl)acetic acid (1a)

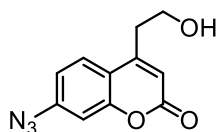
Compound **1a** was prepared following literature procedures.¹⁵ Briefly, 3-aminophenol (10 g, 91.7 mmol) in ethyl acetate (EA; 250 mL) was heated to reflux for 30 min. Ethyl chloroformate (9.6 mL, 100.9 mmol) was added to the refluxing mixture dropwise over 30 min. The reaction mixture was further heated to reflux for 1 h. The mixture was filtered while hot and the filtrate was evaporated to dryness. Isopropanol was added to the off-white residue, and the dissolved solution was kept at 4 °C overnight to obtain the carbamate product as a grey crystal (11.6 g). To a mixture of the grey crystal and diethyl-1,3-acetone dicarboxylate (12.8 mL, 70.6 mmol) was added 70% H₂SO₄ dropwise. After stirring overnight, the solution was poured into 300 mL of ice water. The precipitate was filtered to give the desired product as a light pink solid. The crude solid was dissolved in an aqueous solution (200 mL) of sodium hydroxide (25.7 g, 641.9 mmol). The mixture was stirred under reflux for 2 h and then cooled to 0 °C. The pH was adjusted to 2.0 by dropwise addition of concentrated H₂SO₄. A light-yellow precipitate was observed. The reaction mixture was cooled to 0 °C and the precipitate was

filtered off to give the desired product **1a** (8.6 g, 43% yield) as a light-yellow solid. **1a** was directly used in the next step without further purification. ^1H NMR (500 MHz, CD_3OD) δ 7.76 (d, J = 9.3 Hz, 1H), 7.10 – 7.08 (m, 1H), 7.08 (s, 1H), 6.39 (s, 1H), 3.90 (d, J = 0.6 Hz, 2H). ^{13}C NMR (126 MHz, CD_3OD) δ 172.4, 162.3, 156.1, 151.1, 145.8, 128.0, 117.6, 116.8, 116.3, 108.1, 38.4.



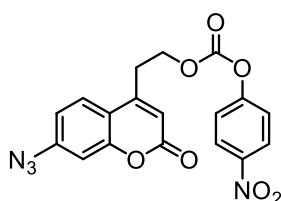
7-amino-4-(2-hydroxyethyl)-2H-chromen-2-one (**2a**)

To a solution of **1a** (8.6 g, 39.4 mmol) in 300 mL of anhydrous THF was added a solution of borane in THF (1.0 M, 59.1 mL) dropwise at 0 °C under a N_2 atmosphere. The mixture was allowed to reach room temperature and stirred for 8 hours. The reaction mixture was cooled to 0 °C and then 20 mL of water were added. The solvent was evaporated under vacuum. The residue was dissolved in EtOAc, washed with water, dried over anhydrous Na_2SO_4 , filtered, and evaporated to dryness to give a solid residue. After purification by column chromatography ($\text{CHCl}_3/\text{MeOH}$ = 30:1 v/v), **2a** was obtained as a white solid (4.1 g, 51% yield). ^1H NMR (400 MHz, CD_3OD) δ 7.49 (d, J = 8.7 Hz, 1H), 6.65 (dd, J = 8.7, 2.2 Hz, 1H), 6.52 (d, J = 2.2 Hz, 1H), 6.00 (s, 1H), 3.85 (t, J = 6.5 Hz, 2H), 2.95 (t, J = 6.5 Hz, 2H). ^{13}C NMR (101 MHz, CD_3OD) δ 164.6, 157.5, 157.1, 154.5, 127.0, 113.1, 110.6, 108.9, 100.8, 61.6, 36.0. HRMS calcd for $\text{C}_{11}\text{H}_{11}\text{NO}_3$ $[\text{M}+\text{H}]^+$: 206.0817; found: 206.0812.



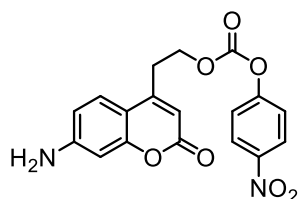
7-azido-4-(2-hydroxyethyl)-2H-chromen-2-one (**3a**)

To a cooled solution of **2a** (4.1 g, 20.1 mmol) in 20 % H_2SO_4 (80 mL) was added a solution of NaNO_2 (4.2 g, 60.3 mmol) in water (4 mL) dropwise at 0 °C. The reaction temperature was maintained at 0–5 °C. After stirring for 30 min, a solution of NaN_3 (5.2 g, 80.4 mmol) in water (4 mL) was added dropwise into the above mixture at 0 °C. The resulting reaction mixture was stirred overnight and then extracted with EtOAc (3 × 100 mL). The organic layer was washed with brine and dried with anhydrous Na_2SO_4 . After filtration, the organic phase was concentrated under vacuum. The crude product was purified by column chromatography ($\text{CHCl}_3/\text{MeOH}$ = 60:1 v/v) to obtain **3a** as a light-yellow solid (4.1 g, 89% yield). ^1H NMR (400 MHz, CD_3OD) δ 7.81 (d, J = 8.6 Hz, 1H), 7.06 (dd, J = 8.6, 2.3 Hz, 1H), 7.02 (d, J = 2.2 Hz, 1H), 6.31 (s, 1H), 3.89 (t, J = 6.3 Hz, 2H), 3.01 (t, J = 6.1 Hz, 2H). ^{13}C NMR (101 MHz, CD_3OD) δ 162.5, 156.1, 155.6, 145.5, 127.8, 117.8, 116.7, 114.6, 108.1, 61.1, 35.7. HRMS calcd for $\text{C}_{11}\text{H}_9\text{N}_3\text{O}_3$ $[\text{M}+\text{H}]^+$: 232.0722; found: 232.0717.



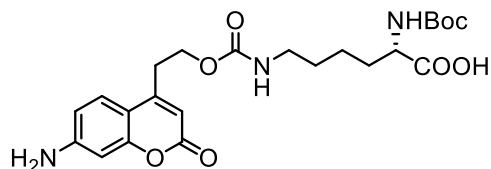
2-(7-azido-2-oxo-2H-chromen-4-yl)ethyl (4-nitrophenyl) carbonate (**4a**)

To a stirring solution of compound **3a** (4.1 g, 17.9 mmol) in DCM (100 mL) at 0 °C was added a solution of triethylamine (TEA; 3.7 mL, 26.9 mmol) and nitrophenyl chloroformate (5.4 g, 26.9 mmol) in DCM (20 mL) under a N₂ atmosphere. The reaction was then allowed to warm to room temperature until consumption of the starting material **3a** as revealed by TLC. The reaction mixture was washed with a saturated aqueous solution of NaHCO₃ and brine. The organic layer was dried over anhydrous Na₂SO₄, filtered, and evaporated under reduced pressure. The crude product was purified by column chromatography (CHCl₃/MeOH = 100:1 v/v) to obtain **4a** (3.3 g, 47% yield) as a yellow solid. ¹H NMR (400 MHz, CDCl₃) δ 8.28 (d, *J* = 9.2 Hz, 2H), 7.64 (d, *J* = 8.3 Hz, 1H), 7.36 (d, *J* = 9.2 Hz, 2H), 7.00 (s, 1H), 6.98 (d, *J* = 2.2 Hz, 1H), 6.33 (s, 1H), 4.61 (t, *J* = 6.6 Hz, 2H), 3.23 (t, *J* = 6.4 Hz, 2H). ¹³C NMR (101 MHz, CDCl₃) δ 160.1, 155.3, 155.1, 152.5, 150.5, 145.7, 144.6, 125.6, 125.5, 121.9, 115.9, 115.8, 114.6, 107.7, 66.2, 30.8. HRMS calcd for C₁₈H₁₄N₂O₇ [M+H]⁺: 397.0784; found: 391.0781.



2-(7-amino-2-oxo-2H-chromen-4-yl)ethyl (4-nitrophenyl) carbonate (**5a**)

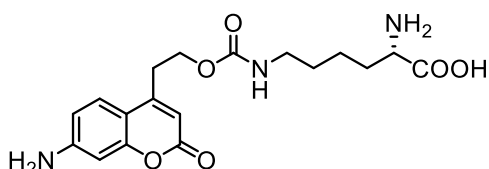
To a solution of compound **4a** (3.3 g, 8.4 mmol) in THF (90 mL) and water (10 mL) was added triphenylphosphine (2.6 g, 10.1 mmol). The reaction mixture was stirred at room temperature for 1 h and then diluted with water and EtOAc. The organic layer was separated, washed with brine, dried over anhydrous Na₂SO₄, filtered, and concentrated under reduced pressure. The obtained crude compound was re-dissolved in 0.01 M HCl (10 mL) and stirred at 60 °C for 15 min. The reaction mixture was extracted with EtOAc. The organic layer was washed with brine, dried over anhydrous Na₂SO₄, filtered, and concentrated under reduced pressure. The resulting crude product was carefully washed with DCM (5 mL) to provide compound **5a** (2.7 g, 87% yield) as a pure yellow powder without further purification. ¹H NMR (400 MHz, *d*⁶-DMSO) δ 8.28 (d, *J* = 9.2 Hz, 2H), 7.53 – 7.50 (m, 2H), 7.50 (s, 1H), 6.56 (dd, *J* = 8.7, 2.1 Hz, 1H), 6.42 (d, *J* = 2.1 Hz, 1H), 6.14 (s, 2H), 5.98 (s, 1H), 4.52 (t, *J* = 6.4 Hz, 2H), 3.13 (t, *J* = 6.3 Hz, 2H). ¹³C NMR (101 MHz, *d*⁶-DMSO) δ 160.6, 155.7, 155.2, 153.2, 152.8, 151.8, 145.2, 125.9, 125.3, 122.5, 111.3, 107.8, 107.7, 98.7, 67.0, 29.9. HRMS calcd for C₁₈H₁₄N₂O₇ [M+H]⁺: 371.0879; found: 371.0876.



*N*⁶-((2-(7-amino-2-oxo-2H-chromen-4-yl)ethoxy)carbonyl)-*N*²-(*tert*-butoxycarbonyl)-*L*-lysine (**6a**)

To a stirred solution of *N*²-Boc-*L*-Lys (2.7 g, 11.0 mmol) and *N,N*-diisopropylethylamine (DIPEA; 2.4 mL, 14.6 mmol) in DMF (10 mL) was added a solution of compound **5a** (2.7 g, 7.3 mmol) in DMF (50 mL) dropwise. The reaction mixture was stirred at room temperature overnight and concentrated by evaporation under reduced pressure. The residue was taken up in water and EtOAc. The aqueous phase was carefully acidified with concentrated HCl, and extracted with EtOAc (3 × 50 mL). The combined organic layers were washed with brine

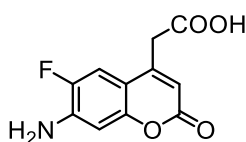
and dried over anhydrous Na₂SO₄. The solvent was evaporated under reduced pressure and the crude product was purified by column chromatography (CHCl₃/MeOH = 20:1 v/v) to provide compound **6a** (2.5 g, 71% yield) as a very viscous yellow oil. ¹H NMR (400 MHz, CD₃OD) δ 7.51 (d, *J* = 8.7 Hz, 1H), 6.65 (dd, *J* = 8.7, 2.2 Hz, 1H), 6.51 (d, *J* = 2.1 Hz, 1H), 5.98 (s, 1H), 4.32 (t, *J* = 6.4 Hz, 2H), 4.06 (dd, *J* = 8.9, 4.7 Hz, 1H), 3.13 – 3.06 (m, 2H), 3.06 – 2.97 (m, 2H), 1.88 – 1.55 (m, 2H), 1.54 – 1.34 (m, 13H). ¹³C NMR (101 MHz, CD₃OD) δ 176.2, 164.4, 158.7, 158.1, 157.4, 156.2, 154.4, 127.0, 113.3, 110.5, 109.1, 100.8, 80.5, 63.8, 54.8, 41.4, 32.6, 32.4, 30.4, 28.7, 24.1. HRMS calcd for C₂₃H₃₁N₃O₈ [M+Na]⁺: 500.2009; found: 500.2005.



N⁶-((2-(7-amino-2-oxo-2H-chromen-4-yl)ethoxy)carbonyl)-L-lysine (ACouK)

To a solution of compound **6a** (2.5 g, 5.2 mmol) in anhydrous DCM (5 mL) was added TFA (5 mL) under a N₂ atmosphere. After stirring for 1 h at room temperature, the reaction mixture was concentrated under reduced pressure to remove the solvent and TFA. The crude product was dissolved in MeOH and precipitated with Et₂O under vigorous stirring. The precipitate was collected, re-dissolved in MeOH, and precipitated again with Et₂O. The progress was repeated twice to furnish the TFA salt of **ACouK** (1.6 g, 81% yield) as a white solid. ¹H NMR (300 MHz, CD₃OD) δ 7.53 (d, *J* = 8.7 Hz, 1H), 6.66 (dd, *J* = 8.7, 1.9 Hz, 1H), 6.51 (d, *J* = 1.8 Hz, 1H), 5.98 (s, 1H), 4.34 (t, *J* = 6.2 Hz, 2H), 3.68 (t, *J* = 6.1 Hz, 1H), 3.14 – 3.09 (m, 2H), 3.06 – 2.98 (m, 2H), 1.93-1.80 (m, 2H), 1.58 – 1.33 (m, 4H). ¹³C NMR (101 MHz, CD₃OD) δ 173.3, 164.5, 158.8, 157.4, 156.3, 154.7, 127.0, 113.3, 110.4, 109.0, 100.7, 63.8, 55.1, 41.3, 32.6, 31.6, 30.5, 23.4. HRMS calcd for C₁₈H₂₃N₃O₆ [M+H]⁺: 378.1665; found: 378.1659.

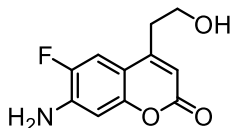
Synthesis of AFCouK



2-(7-amino-6-fluoro-2-oxo-2H-chromen-4-yl)acetic acid (1b)

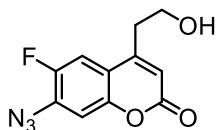
Compound **1b** was prepared following literature procedures.¹⁵ Briefly, 3-amino-4-fluorophenol (10 g, 78.7 mmol) in EtOAc (250 mL) was heated to reflux for 30 min. Ethyl chloroformate (8.2 mL, 86.6 mmol) was added to the refluxing mixture dropwise over 30 min. The reaction mixture was further heated to reflux for 1 h. The mixture was filtered while hot and the filtrate was evaporated to dryness. Isopropanol was added to the off-white residue, and the dissolved solution was kept at 4 °C overnight to obtain the carbamate product as a grey crystal (11.1 g). To a mixture of the grey crystal and diethyl-1,3-acetone dicarboxylate (55.3 mL, 61.5 mmol) was added 70% H₂SO₄ dropwise. After stirring overnight, the solution was poured into 300 mL of ice water. The precipitate was filtered to give the desired product as a light pink solid. The crude solid was dissolved in an aqueous solution (200 mL) of sodium hydroxide (22.4 g, 559 mmol). The mixture was stirred under reflux for 2 h and then cooled to 0 °C. The pH was adjusted to 2.0 by dropwise addition of concentrated H₂SO₄. A light-yellow precipitate was observed. The mixture was cooled to 0 °C and the precipitate was filtered off to give the desired product **1b** (9.7 g, 52% yield) as a light-yellow solid. **1b** was directly used

in the next reaction without further purification. ^1H NMR (400 MHz, d^6 -DMSO) δ 7.35 (d, J = 12.1 Hz, 1H), 6.62 (d, J = 7.7 Hz, 1H), 6.25 (s, 2H), 6.09 (s, 1H), 3.76 (s, 2H). ^{13}C NMR (101 MHz, d^6 -DMSO) δ 160.5, 153.6, 153.5, 151.3, 148.4, 146.1, 143.1, 141.3, 141.1, 110.5, 110.3, 108.9, 108.0, 107.9, 100.8, 100.7, 18.2. ^{19}F NMR (376 MHz, d^6 -DMSO) δ -138.5.



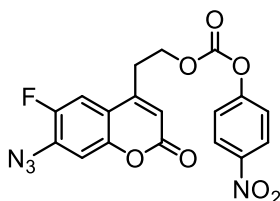
7-amino-6-fluoro-4-(2-hydroxyethyl)-2H-chromen-2-one (**2b**)

To a solution of **1b** (9.7 g, 40.9 mmol) in 300 mL of anhydrous THF at 0 °C was added a solution of borane in THF (1.0 M, 61 mL) dropwise under a N_2 atmosphere. The mixture was allowed to warm to room temperature and stirred for 8 hours. The reaction mixture was cooled to 0 °C and then 20 mL of water were added. The solvent was evaporated under vacuum. The resulting residue was dissolved in EtOAc, washed with water, dried over anhydrous Na_2SO_4 , filtered, and evaporated to dryness to give a solid residue. After purification by column chromatography ($\text{CHCl}_3/\text{MeOH}$ = 30:1 v/v), compound **2b** was obtained as a white solid (3.6 g, 39% yield). ^1H NMR (400 MHz, d^6 -DMSO) δ 7.45 (d, J = 12.3 Hz, 1H), 6.62 (d, J = 7.7 Hz, 1H), 6.16 (s, 2H), 6.00 (s, 1H), 4.77 (t, J = 5.4 Hz, 1H), 3.67 (q, J = 6.1 Hz, 2H), 2.80 (t, J = 6.3 Hz, 2H). ^{13}C NMR (101 MHz, d^6 -DMSO) δ 160.5, 154.8, 154.7, 151.6, 148.4, 146.1, 141.1, 140.9, 110.4, 110.2, 109.0, 107.6, 107.5, 101.0, 100.9, 59.6, 34.6. ^{19}F NMR (376 MHz, d^6 -DMSO) δ -138.4. HRMS calcd for $\text{C}_{11}\text{H}_{10}\text{FNO}_3$ [$\text{M}+\text{H}$] $^+$: 224.0723; found: 224.0719.



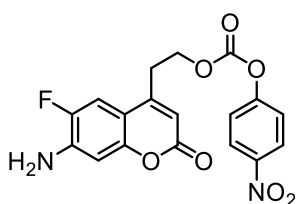
7-azido-6-fluoro-4-(2-hydroxyethyl)-2H-chromen-2-one (**3b**)

To a cooled solution of **2b** (3.6 g, 16.0 mmol) in 20 % H_2SO_4 (100 mL) was added a solution of NaNO_2 (2.2 g, 32.0 mmol) in water (3 mL) dropwise at 0 °C. The reaction temperature was maintained at 0–5 °C. After stirring for 30 min, a solution of NaN_3 (2.8 g, 43.2 mmol) in water (3 mL) was added dropwise into the mixture at 0 °C. The resulting reaction mixture was stirred overnight and extracted with EtOAc (3 \times 100 mL). The organic layer was washed with brine and then dried over anhydrous Na_2SO_4 . After filtration, the organic phase was concentrated under vacuum. The crude residue was purified by column chromatography ($\text{CHCl}_3/\text{MeOH}$ = 60:1 v/v) to obtain compound **3b** (2.6 g, 65% yield) as a light-yellow solid. ^1H NMR (300 MHz, d^6 -DMSO) δ 7.75 (d, J = 11.9 Hz, 1H), 7.33 (d, J = 7.3 Hz, 1H), 6.33 (s, 1H), 4.83 (t, J = 5.5 Hz, 1H), 3.70 (q, J = 6.0 Hz, 2H), 2.87 (t, J = 6.1 Hz, 2H). ^{13}C NMR (75 MHz, d^6 -DMSO) δ 159.4, 153.8, 153.7, 151.8, 150.0, 149.9, 148.5, 131.2, 131.0, 116.7, 116.6, 114.3, 112.6, 112.3, 109.1, 59.3, 34.4. ^{19}F NMR (376 MHz, d^6 -DMSO) δ -131.1. HRMS calcd for $\text{C}_{11}\text{H}_8\text{FN}_3\text{O}_3$ [$\text{M}+\text{H}$] $^+$: 250.0628; found: 250.0623.



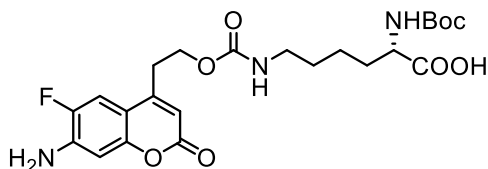
2-(7-azido-6-fluoro-2-oxo-2H-chromen-4-yl)ethyl (4-nitrophenyl) carbonate (**4b**)

To a stirring solution of compound **3b** (2.6 g, 10.4 mmol) in DCM (80 mL) at 0 °C was added a solution of triethylamine (TEA; 2.2 mL, 15.6 mmol) and nitrophenyl chloroformate (3.1 g, 15.6 mmol) in DCM (20 mL) under a N₂ atmosphere. The reaction was then allowed to warm to room temperature until consumption of the starting material **3b** as revealed by TLC. The reaction mixture was washed with a saturated aqueous solution of NaHCO₃ and brine. The organic layer was dried over anhydrous Na₂SO₄, filtered, and evaporated under reduced pressure to obtain compound **4b** (1.5 g, 35% yield) as a yellow solid without further purification. ¹H NMR (400 MHz, *d*⁶-DMSO) δ 8.29 (d, *J* = 9.1 Hz, 2H), 7.89 (d, *J* = 11.9 Hz, 1H), 7.52 (d, *J* = 9.1 Hz, 2H), 7.44 (d, *J* = 7.2 Hz, 1H), 6.50 (s, 1H), 4.56 (t, *J* = 6.1 Hz, 2H), 3.24 (t, *J* = 6.1 Hz, 2H). ¹³C NMR (101 MHz, *d*⁶-DMSO) δ 159.2, 155.2, 151.7, 151.6(5), 151.6(3), 151.4, 150.0(1), 150.0(0), 149.0, 145.2, 131.5, 131.4, 125.4, 122.5, 116.1, 116.0, 114.8, 112.4, 112.2, 109.3, 66.6, 29.9. ¹⁹F NMR (376 MHz, *d*⁶-DMSO) δ -130.7. HRMS calcd for C₁₈H₁₁FN₄O₇ [M+H]⁺: 415.0690; found: 415.0685.



2-(7-amino-6-fluoro-2-oxo-2H-chromen-4-yl)ethyl (4-nitrophenyl) carbonate (**5b**)

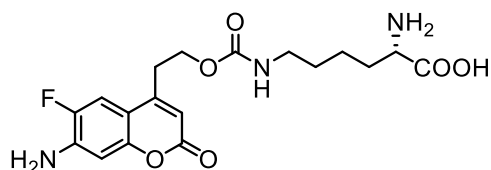
To a solution of compound **4b** (1.5 g, 3.6 mmol) in THF (45 mL) and water (5 mL) was added triphenylphosphine (1.1 g, 4.3 mmol). The reaction mixture was stirred at room temperature for 1 h and then diluted with water and EtOAc. The organic layer was separated, washed with brine, dried over anhydrous Na₂SO₄, filtered, and concentrated under reduced pressure. The obtained crude compound was re-dissolved in 0.01 M HCl (10 mL) and stirred at 60 °C for 15 min. The reaction mixture was extracted with EtOAc. The organic layer was washed with brine, dried over anhydrous Na₂SO₄, filtered, and concentrated under reduced pressure. The resulting crude product was carefully washed with DCM (5 mL) to provide compound **5b** (1.2 g, 85% yield) as a pure yellow powder without further purification. ¹H NMR (300 MHz, *d*⁶-DMSO) δ 8.30 (d, *J* = 9.2 Hz, 2H), 7.56 (d, *J* = 11.8 Hz, 2H), 7.52 (d, *J* = 9.1 Hz, 2H), 6.64 (d, *J* = 7.7 Hz, 1H), 6.25 (s, 2H), 6.11 (s, 1H), 4.52 (t, *J* = 6.2 Hz, 2H), 3.14 (t, *J* = 6.2 Hz, 2H). ¹³C NMR (75 MHz, *d*⁶-DMSO) δ 160.3, 155.2, 152.7, 152.6, 151.8, 151.6, 148.9, 145.7, 145.2, 141.4, 141.2, 125.4, 122.6, 110.4, 110.1, 109.3, 107.1, 107.0, 101.0, 100.9, 66.9, 30.0. ¹⁹F NMR (376 MHz, *d*⁶-DMSO) δ -138.1. HRMS calcd for C₁₈H₁₃FN₂O₇ [M+H]⁺: 389.0785; found: 389.0780.



N⁶-((2-(7-amino-6-fluoro-2-oxo-2H-chromen-4-yl)ethoxy)carbonyl)-N²-(tert-butoxycarbonyl)-L-lysine (**6b**)

To a stirred solution of N⁶-Boc-L-Lys (1.2 g, 4.7 mmol) and *N,N*-diisopropylethylamine (DIPEA; 1 mL, 6.2 mmol) in DMF (5 mL) was added a solution of compound **5b** (1.2 g, 3.1 mmol) in DMF (20 mL) dropwise. The reaction mixture was stirred at room temperature overnight and concentrated by evaporation under reduced pressure. The residue was taken

up in water and EtOAc. The aqueous phase was carefully acidified with concentrated HCl, and extracted with EtOAc (3 × 50 mL). The combined organic layers were washed with brine and dried over anhydrous Na₂SO₄. The solvent was evaporated under reduced pressure and the crude product was purified by column chromatography (CHCl₃/MeOH = 20:1 v/v) to provide compound **6b** (1.1 g, 74% yield) as a very viscous yellow oil. ¹H NMR (300 MHz, CD₃OD) δ 7.42 (d, *J* = 11.9 Hz, 1H), 6.67 (d, *J* = 7.6 Hz, 1H), 6.07 (s, 1H), 4.33 (t, *J* = 6.3 Hz, 2H), 4.05 (dd, *J* = 8.8, 4.6 Hz, 1H), 3.12 – 3.05 (m, 2H), 3.05 – 2.96 (m, 2H), 1.87 – 1.55 (m, 2H), 1.53 – 1.32 (m, 13H). ¹³C NMR (75 MHz, CD₃OD) δ 176.3, 164.0, 158.7, 158.2, 155.8, 155.7, 153.3, 151.1, 148.0, 143.0, 142.8, 111.0, 110.7, 110.4, 109.7, 109.6, 102.7, 102.6, 80.5, 63.6, 54.8, 41.4, 32.7, 32.4, 30.4, 28.7, 24.1. ¹⁹F NMR (376 MHz, CD₃OD) δ -140.12. HRMS calcd for C₂₃H₃₀FN₃O₈ [M+Na]⁺: 518.1915; found: 518.1913.



N⁶-((2-(7-amino-6-fluoro-2-oxo-2H-chromen-4-yl)ethoxy)carbonyl)-L-lysine (AFCouK)

To a solution of compound **6b** (1.1 g, 2.3 mmol) in anhydrous DCM (5 mL) was added TFA (5 mL) under a N₂ atmosphere. After stirring for 1 h at room temperature, the reaction mixture was concentrated under reduced pressure to remove the solvent and TFA. The crude product was dissolved in MeOH and precipitated with Et₂O under vigorous stirring. The precipitate was collected, re-dissolved in MeOH, and precipitated again with Et₂O. The progress was repeated twice to furnish the TFA salt of **AFCouK** (0.66 g, 73% yield) as a white solid. ¹H NMR (400 MHz, CD₃OD) δ 7.43 (d, *J* = 11.9 Hz, 1H), 6.68 (d, *J* = 7.6 Hz, 1H), 6.07 (s, 1H), 4.34 (t, *J* = 6.2 Hz, 2H), 3.78 (t, *J* = 6.2 Hz, 1H), 3.09 (t, *J* = 6.5 Hz, 2H), 3.04 (t, *J* = 6.2 Hz, 2H), 1.98 – 1.75 (m, 2H), 1.59 – 1.33 (m, 4H). ¹³C NMR (101 MHz, CD₃OD) δ 174.0, 164.0, 158.7, 155.8(8), 155.8(6), 153.3, 150.8, 148.4, 143.1, 142.9, 111.0, 110.8, 110.4, 109.6, 109.5, 102.7, 102.6, 63.6, 55.7, 41.3, 32.7, 31.9, 30.5, 23.5. ¹⁹F NMR (376 MHz, CD₃OD) δ -76.9, -140.2. HRMS calcd for C₁₈H₂₂FN₃O₆ [M+H]⁺: 396.1571; found: 396.1570.

Plasmids and cloning

For *E. coli* transformation, the pBX-MmPyIRS plasmid expressing wild-type PyIRS from *Methanosarcina mazei* was constructed as previously reported.¹⁶ The plasmid pBX-MmPyIRS was mutated at indicated sites with site-directed mutagenesis to produce the PyIRS variants. The pLX-EGFP-Y39TAG plasmid containing the *Methanosarcina mazei* tRNA_{CUA}-Pyl gene under the *lpp* promoter and *rmC* terminator and the EGFP-Y39TAG gene was constructed as previously reported.¹⁶ The EGFP-Y39TAG gene containing a C-terminal 6*His-tag was under the control of a bacteriophage T5 promoter and *t₀* terminator.

To construct the pLX-Ub-Y59TAG-EGFP plasmid, the ubiquitin gene was amplified from the pET28a-Ub plasmid (a kind gift from Prof. Hao Huang at Peking University) and inserted into the pLX-EGFP plasmid upstream of the EGFP gene by Gibson assembly to generate pLX-Ub-EGFP. Site-directed mutagenesis was applied to pLX-Ub-EGFP to generate the pLX-Ub-Y59TAG-EGFP plasmid. The sfGFP and cpsfGFP encoding genes were amplified from the pBad-sfGFP-150TAG plasmid (a kind gift from Prof. Ryan Mehl; Addgene plasmid # 85483) and the pBAD-hsGFP plasmid (a kind gift from Prof. Huiwang Ai; Addgene plasmid # 64911), respectively, and used to replace the EGFP gene in the pLX-Ub-Y59TAG-EGFP

plasmid to create the pLX-Ub-Y59TAG-sfGFP and pLX-Ub-Y59TAG-cpsfGFP plasmids, respectively. The mutations were corrected with site-directed mutagenesis.

To create the pLX-Ub-Y59TAG-sfGFP plasmids with different linkers between Ub-Y59TAG and sfGFP genes, the following linker sequences were inserted into pLX-Ub-Y59TAG-sfGFP between Ub-Y59TAG and sfGFP genes with PCR amplification and Gibson assembly to generate corresponding plasmids. pLX-Ub-Y59TAG-sfGFP-16-1 with linker 16-1: tccggactcagatccgctggcccagctggcccaggaggacgatcgga. pLX-Ub-Y59TAG-sfGFP-16-2 with linker 16-2: atagcatggcctttggctggcccagctggcccaggaggacgatcgga. pLX-Ub-Y59TAG-sfGFP-21 with linker 21: atagcatggcctttgtccggactcagatccgctggcccagctggcccaggaggacgatcgga.

To construct pLX-Ub-Y59TAG-Ub-sfGFP, the G75A/G76A mutation were first introduced into pLX-Ub-sfGFP to generate pLX-Ub-G75A/G76A-sfGFP. Another Ub gene with a Y59TAG mutation was amplified and then inserted into pLX-Ub-G75A/G76A-sfGFP upstream of the Ub-G75A/G76A fragment to create the pLX-Ub-Y59TAG-Ub-sfGFP plasmid.

The pET28a-USP7 and pET28a-OTULIN plasmids encoding USP7 (residue 208-560) and OTULIN, respectively, with *N*-terminal 6*His tags under the T7 promoter were kindly provided by Prof. Hao Huang at Peking University. The pET28a-USP7-C223S plasmid was generated by site-directed mutagenesis on pET28a-USP7. The pGEX-4T-1-GST-tetra-ubiquitin plasmid encoding linear tetra-ubiquitin with an *N*-terminal GST tag followed by a HRV 3C cleavage site under the tac promoter was kindly provided by Prof. Hao Huang at Peking University.

For mammalian cell transfection, the pEF1 α -FLAG-MmPyIRS plasmid was initially developed by Prof. Jason Chin¹⁷ and constructed in the lab previously.¹⁶ The pCMV-EGFP-Y39TAG plasmid was previously developed in the lab.^{16, 18} The desired mutations were introduced into the pEF1 α -FLAG-MmPyIRS plasmid to create pEF1 α -FLAG-ACouKRS.

Screening of MmPyIRS variants for ACouK and AFCouK incorporation

The pLX-EGFP-Y39TAG plasmid was co-transformed with individual pBX-MmPyIRS mutant plasmid into the *E. coli* strain BL21 (DE3). The transformed bacteria cells were grown in LB medium with kanamycin (40 μ g/mL) and chloramphenicol (34 μ g/mL) overnight at 37 °C and then inoculated by 1:100 dilution into fresh LB medium supplemented with kanamycin (40 μ g/mL) and chloramphenicol (34 μ g/mL) at 37 °C. 1 mM ACouK or AFCouK was added into the bacterial culture when OD₆₀₀ reached 0.6. After 0.5 h incubation, 1 mM IPTG was added into the culture to induce the protein expression at 37 °C for 10 h. The EGFP fluorescence intensity of individual bacterial culture was measured on a Biotek Synergy H1 microplate reader and compared with the control culture in the absence of UAA.

Incorporation of fluorescent unnatural amino acids into proteins in *E. coli*

The desired plasmid of interest containing amber TAG codon was co-transformed with the pBX-ACouKRS plasmid into the *E. coli* strain BL21 (DE3). The transformed bacteria cells were grown in LB medium with kanamycin (40 μ g/mL) and chloramphenicol (34 μ g/mL) overnight at 37 °C and then inoculated by 1:100 dilution into fresh LB medium supplemented with kanamycin (40 μ g/mL) and chloramphenicol (34 μ g/mL) at 37 °C. 1 mM ACouK or AFCouK was added into the bacterial culture when OD₆₀₀ reached 0.6. After 0.5 h incubation, 1 mM IPTG was added into the culture to induce the protein expression at 37 °C for 10 h. The cells were harvested and lysed with 4% SDS lysis buffer (4% SDS, 150 mM NaCl, 50 mM triethanolamine pH 7.4) at 95 °C for 5 min. The resulting cell lysates were centrifuged at 16,000g for 5 min at room temperature to remove cellular debris. Protein concentrations were

determined by the BCA assay (Pierce). Finally, the cell lysates were separated on 4-20% SDS-PAGE gels (Genscript Biotech) and analyzed by western blotting and Coomassie Brilliant Blue staining.

For concentration-dependent incorporation of AFCouK in *E. coli*, the pLX-EGFP-Y39TAG plasmid was co-transformed with the pBX-ACouKRS plasmid into the *E. coli* strain BL21 (DE3). The transformed bacteria cells were grown in LB medium with kanamycin (40 µg/mL) and chloramphenicol (34 µg/mL) overnight at 37 °C and then inoculated by 1:100 dilution into fresh LB medium supplemented with kanamycin (40 µg/mL) and chloramphenicol (34 µg/mL) at 37 °C. AFCouK at different concentrations (from 0 mM to 2 mM) was added into the bacterial culture when OD₆₀₀ reached 0.6. EGFP-Y39TAG protein expression was induced and assessed by western blotting and Coomassie Brilliant Blue staining as described above.

Purification of proteins containing fluorescent unnatural amino acids from *E. coli*

For purification of desired proteins, the desired plasmid of interest containing amber TAG codon was co-transformed with the pBX-ACouKRS plasmid into the *E. coli* strain BL21 (DE3). The transformed bacteria cells were grown in LB medium with kanamycin (40 µg/mL) and chloramphenicol (34 µg/mL) overnight at 37 °C and then inoculated by 1:100 dilution into fresh LB medium supplemented with kanamycin (40 µg/mL) and chloramphenicol (34 µg/mL) at 37 °C. 1 mM ACouK, AFCouK, HCouK, or Bock was added into the bacterial culture when OD₆₀₀ reached 0.6. After 0.5 h incubation, 1 mM IPTG was added into the culture to induce the protein expression at 37 °C for 10 h. The cells were harvested and lysed with a sonic disruptor (Scientz, JY92-IIN) in the binding buffer (20 mM Tris-HCl, 500 mM NaCl, 10% glycerol, 10 mM imidazole, pH 8.0) containing protease inhibitor cocktails, PMSF, deoxyribonuclease I, and lysozyme. The supernatant after centrifugation was then purified by Ni-NTA Sefinose Resin 6FF (Sangon Biotech, cat#C600033-0025) according to the manufacturer's protocol and eluted with the elution buffer (binding buffer supplemented with 250 mM imidazole). The purified protein was stored at -80 °C.

Mass spectrometry analysis of purified proteins

The purified proteins were desalted with 10 kDa Amicon centrifugal filters (Millipore, cat#MRCPR010), washed three times with water, and reconstituted into 0.01% ammonia solution. The resulting samples were analyzed on a Q Exactive Focus LC-MS/MS system (Thermo Fisher Scientific) equipped with a nano-ESI ionization source. The mass spectra were deconvoluted with the BioPharma Finder software (Thermo Fisher Scientific).

Mammalian cell culture and transfection

HEK293T cells were obtained from ATCC. Cells were grown in DMEM (Dulbecco's modified Eagle's medium; Cytiva, cat#SH30243.01) supplemented with 10% FBS (fetal bovine serum; Biological Industries, cat#04-001-1ACS) in a humidified incubator at 37 °C with 5% CO₂. For transfection, cells were grown on cell culture dishes or plates to 70% confluence and transfected with indicated plasmids using PEI (Polysciences) for 18–24 h in cell growth media.

Incorporation of fluorescent unnatural amino acids into proteins in mammalian cells

HEK293T cells were seeded on 12-well plates (Corning) and cultured overnight in 1 mL of growth media. On the next day cells were co-transfected with the desired plasmid of interest containing an amber TAG codon (0.65 µg per well) and the PylRS plasmid (0.35 µg

per well) using PEI (2.5 µg per well) in complete cell growth media in the absence or presence of UAA (0.5 mM unless otherwise stated). For expression of ACouK or AFCouK modified proteins, pEF1α-FLAG-ACouKRS was used, while pEF1α-FLAG-MmPylRS was used for incorporation of BockK. After 24 h transfection, the cells were lysed with 4% SDS lysis buffer containing Roche protease inhibitor and benzonase by sonication and vortexing. The resulting cell lysates were centrifuged at 16,000g for 5 min at room temperature to remove cellular debris. Protein concentrations were determined by the BCA assay (Pierce). Finally, the cell lysates were separated on 4-20% SDS-PAGE gels (Genscript Biotech) and analyzed by western blotting. Alternatively, cells were imaged in FluoroBrite DMEM (Thermo Scientific) on an Olympus inverted fluorescence microscope. For quantification of fluorescence images, at least three fields of view per dish were randomly selected for every fluorescence imaging experiment. The fluorescence intensity of every image was quantified in ImageJ and grouped for statistical analysis.

Photophysical characterization of fluorescent unnatural amino acids and proteins

For the photophysical characterization of fluorescent unnatural amino acids, HCouK, ACouK, and AFCouK were dissolved in DMSO as the 500 mM stock solutions. UV-Vis absorption spectra and fluorescence spectra of HCouK, ACouK, and AFCouK were recorded on a Biotek Synergy H1 microplate reader with a 10 µM concentration in KCl-HCl (pH = 2), citric acid-Na₂HPO₄ (pH = 2.5, 3.0, 3.5, 4.0, 4.5, 5.0, 5.5, 6.0, 6.5, and 7.0), Tris HCl-Tris base (pH = 7.5, 8.0, 8.5, and 9.0), or Na₂CO₃-NaHCO₃ (pH = 9.5, 10.0, 10.5, and 11.0) buffer solutions. The quantum yields of HCouK, ACouK, and AFCouK were determined in PBS (pH = 7.4) relative to quinine sulfate in 0.5 M H₂SO₄ ($\Phi_F = 0.546$). For photostability measurements, HCouK, ACouK, and AFCouK were diluted to an absorbance of 0.05 absorbance units at 365 nm. 3 mL of these solutions were irradiated in a Spectrolinker XL-1000 Series UV Crosslinker with a 365 nm light source. From the irradiated solutions, 200 µL was taken out and kept in a light tight container at the following timepoints: 0, 2, 4, 8, 12, 15, 20, 30, 45, and 60 minutes. At the end of the irradiation, the fluorescence intensities were measured using a Biotek Synergy H1 microplate reader. Readings were normalized to their 0 minute fluorescence values. The excitation at 350 nm was used for fluorescence measurements, unless otherwise stated.

For the photophysical characterization of fluorescent proteins, the purified EGFP-Y39ACouK, EGFP-Y39AFCouK, EGFP-Y39HCouK and EGFP-BockK proteins were diluted to 0.5 µM with buffers at pH 7.4 or 2.0. The fluorescence emission spectra were recorded with excitation at 350 nm.

For the selection of GFP variants as FRET receptors, the fluorescence spectra of Ub-Y59AFCouK-EGFP, Ub-Y59AFCouK-sfGFP, and Ub-Y59AFCouK-cpsfGFP were recorded at 0.5 µM concentrations in PBS (pH 7.4). For optimization of the Ub-Y59AFCouK-sfGFP fusion protein linkers, the fluorescence spectra were recorded at 0.5 µM concentrations in PBS (pH 7.4) as above.

Fluorescence imaging in live mammalian cells

HEK293T cells were seeded on poly-D-lysine-coated 12-well plates (Corning) and cultured overnight in 1 mL of growth media. On the next day cells were co-transfected with plasmids of pEF1α-FLAG-ACouKRS (0.35 µg per well) and pCMV-EGFP-Y39TAG (0.65 µg per well) using PEI (2.5 µg per well) in complete cell growth media in the presence of AFCouK (0.5 mM). After 24 h incubation, cells were washed with DMEM three times over 6 h to remove

the excess amount of AFCouK. Cells were then imaged in FluoroBrite DMEM (Thermo Scientific) on a Nikon A1R confocal fluorescence microscope. For the coumarin channel, the 405 nm laser was used as the excitation, and emission was collected between 410 nm to 480 nm. For the FRET channel, the 405 nm laser was used as the excitation, and emission was collected between 500 nm to 570 nm. For the EGFP channel, the 488 nm laser was used as the excitation, and emission was collected between 500 nm to 570 nm. In a control experiment, HEK293T cells were co-transfected with plasmids of pEF1 α -FLAG-Mm-PylRS and pCMV-EGFP-Y39TAG in the presence of Bock (0.1 mM) and processed as above.

Detection of deubiquitinase activities of USP7 and OTULIN by SDS-PAGE

For the purification of USP7, USP7-C223S, and OTULIN proteins, the corresponding plasmids were transformed into *E. coli* strain BL21 (DE3) and expression was induced by the addition of 1 mM IPTG at 37°C for 8 h. The USP7, USP7-C223S, and OTULIN proteins were purified by Ni-NTA Sefinose Resin 6FF (Sangon Biotech, cat#C600033-0025) as described above. For the purification of linear tetra-ubiquitin, the GST-tetra-ubiquitin plasmid was transformed into *E. coli* strain BL21 (DE3) and expression was induced by the addition of 1 mM IPTG at 37°C for 8 h. GST-tetra-ubiquitin was purified by BeyoGold™ GST-tag Purification Resin (Beyotime) and the GST tag was removed by HRV 3C protease (Sangon Biotech).

For the detection of the deubiquitinase activity of USP7, cleavage of the purified Ub-Y59AFCouK-sfGFP-21 protein was carried out by incubating the protein (10 μ M) with USP7 (50 nM) in DUB buffer (20 mM Tris-HCl, 150 mM NaCl, 1 mM DTT, 0.5 mM EDTA, pH 7.4) at 37 °C for 6 h. Samples were resolved by SDS-PAGE, imaged by UV trans illumination for in-gel coumarin fluorescence analysis, and then stained with Coomassie Brilliant Blue.

For the detection of the deubiquitinase activity of OTULIN, cleavage of the purified Ub-Y59AFCouK-Ub-sfGFP protein was carried out by incubating the protein (10 μ M) with OTULIN (5 nM) in DUB buffer at 37 °C for 6 h. Samples were resolved by SDS-PAGE, imaged by UV trans illumination for in-gel coumarin fluorescence analysis, and then stained with Coomassie Brilliant Blue.

For the validation of the inhibition effects of TCID and USP30 inhibitor 18 for OTULIN activity, TCID and USP30 inhibitor 18 at varying concentrations were pre-incubated with OTULIN (5 nM) in DUB buffer at 37 °C for 30 min. Next, the enzymatic reactions were initiated by addition of 10 μ M M1-linked linear tetra-ubiquitin (Ub4). After incubation at 37 °C for 6 h, samples were resolved by SDS-PAGE and stained with Coomassie Brilliant Blue.

Detection of deubiquitinase activities of USP7 and OTULIN by fluorescence

For the detection of the deubiquitinase activity of USP7 by fluorescence, USP7-catalyzed enzymatic reactions were conducted in 96-well optical-bottom black plates (Corning, # 3603). The purified Ub-Y59AFCouK-sfGFP proteins (0.5 μ M) were treated with USP7 at varying concentrations (0–64 nM) in DUB buffer (100 μ L) at 37 °C. Fluorescence intensities of the solutions were measured at 440 nm and 510 nm with 350 nm excitation every 20 min over a period of 120 min. After 120 min reaction, the fluorescence spectra were collected with 350 nm excitation.

For the detection of the deubiquitinase activity of OTULIN by fluorescence, OTULIN-catalyzed enzymatic reactions were conducted in 96-well optical-bottom black plates (Corning, # 3603). The purified Ub-Y59AFCouK-Ub-sfGFP protein (0.5 μ M) was treated with OTULIN at varying concentrations (0–4 nM) in DUB buffer (100 μ L) at 37 °C. Fluorescence intensities of

the solutions were measured at 440 nm and 510 nm with 350 nm excitation every 20 min over a period of 120 min. After 120 min reaction, the fluorescence spectra were collected with 350 nm excitation.

For the evaluation of the selectivity of Ub-Y59AFCouK-Ub-sfGFP towards OTULIN, the purified Ub-Y59AFCouK-Ub-sfGFP protein (0.5 μ M) was treated with USP7 at varying concentrations (0–64 nM) and processed as described above.

Screening of deubiquitinase inhibitors by FRET-based fluorescence detection

Forty known DUB inhibitors and inhibitor candidates (Table S2) were purchased from MedChemExpress. The individual inhibitors at two different concentrations (1 μ M and 10 μ M) in duplicate were pre-incubated with USP7 (50 nM) and OTULIN (5 nM) in DUB buffer (20 μ L) at 37 °C for 30 min in 96-well optical-bottom black plates (Corning, # 3603). Next, the corresponding purified proteins, i.e., Ub-Y59AFCouK-sfGFP-21 and Ub-Y59AFCouK-Ub-sfGFP (0.5 μ M), were added and incubated at 37 °C for 120 min. Fluorescence intensities of each well were measured at 440 nm and 510 nm with 350 nm excitation.

The inhibition effect of every compound was calculated by the following equation:

$$\text{Inhibition effect (\%)} = \frac{AC - X}{AC - NC} \times 100\%,$$

where “X” represents the FRET ratio ($F_{440 \text{ nm}}/F_{510 \text{ nm}}$) for each well in the presence of an inhibitor, “AC” is the FRET ratio ($F_{440 \text{ nm}}/F_{510 \text{ nm}}$) for the active control in the absence of any inhibitors (DUB + substrate probe + DMSO), and “NC” is the FRET ratio ($F_{440 \text{ nm}}/F_{510 \text{ nm}}$) for the negative control without DUB (substrate probe + DMSO). The inhibition data are shown as mean values of duplicates and visualized by heatmap using GraphPad prism 8.0.

For measuring the IC_{50} s of inhibitors for USP7 and OTULIN, the potential inhibitors at varying concentrations were pre-incubated with USP7 (50 nM) or OTULIN (5 nM) in DUB buffer (20 μ L) at 37 °C for 30 min in 96-well optical-bottom black plates (Corning, # 3603). Next, the corresponding purified proteins, i.e., Ub-Y59AFCouK-sfGFP-21 and Ub-Y59AFCouK-Ub-sfGFP (0.5 μ M), were added and incubated at 37 °C for 120 min. Fluorescence intensities of each well were measured at 440 nm and 510 nm with 350 nm excitation.

The DUB activity was calculated by the following equation:

$$\text{DUB activity (\%)} = \frac{X - NC}{AC - NC} \times 100\%,$$

where “X” represents the FRET ratio ($F_{440 \text{ nm}}/F_{510 \text{ nm}}$) for each well in the presence of an inhibitor, “AC” is the FRET ratio ($F_{440 \text{ nm}}/F_{510 \text{ nm}}$) for the active control in the absence of any inhibitors (DUB + substrate probe + DMSO), and “NC” is the FRET ratio ($F_{440 \text{ nm}}/F_{510 \text{ nm}}$) for the negative control without DUB (substrate probe + DMSO). The data were fitted with a four-parameter “[inhibitor] vs. response - variable slope” model using GraphPad prism 8.0 and IC_{50} s were calculated by fitting into this model. The data points are shown as mean values \pm s. d., $n = 3$.

Western blotting

SDS-PAGE gels were generally transferred to nitrocellulose membranes using Biorad Trans-Blot Turbo Transfer System (25 V, 30 min). The membranes were blocked with PBST (0.05% Tween-20 in PBS) containing 5% nonfat milk for 30 min at room temperature and incubated with primary antibodies at 4 °C overnight. Membranes were washed with PBST three times and developed using Tanon ECL substrates. Membranes were imaged with a Chemidoc MP imaging system (Biorad).

Anti-6*His-HRP (HRP-66005, 1:5000 dilution), anti-GFP-HRP (HRP-66002, 1:1000 dilution), anti- α -tubulin-HRP (HRP-66031, 1:5000 dilution), and anti- β -actin-HRP (HRP-60008, 1:5000 dilution) antibodies for Western blotting were purchased from Proteintech.

Quantification and statistical analysis

Data were generally presented as mean \pm standard deviation determined from biological replicates. The method for determining error bars and significance is indicated in the corresponding figure legends. Statistical analysis was performed with GraphPad Prism 8.

Protein sequences

EGFP-Y39TAG sequence (* denotes the UAA site):

MVSKGEELFTGVVPILVELDGDVNGHKFSVSGEGEGDAT*GKLT LKFICTTGKLPVP
WPTLVTTLT YGVQCFSRYPDHMKQHDFFKSAMPEGYVQERTIFFKDDGNYKTRAEVKFEG
DTLVNRIELKGIDFKEDGNILGHKLEYNYNSHNVYIMADKQKNGIKVNFKIRHNIEDGGSVQLA
DHYQQNTPIGDGPVLLPDNHYLSTQSALS KDPNEKRDHMLLEFVTAAGITLGMDELYKRS
HHHHHH

Ub-Y59TAG-EGFP sequence (* denotes the UAA site):

MQIFVKLT LTKGTITLEVEPSDTIENVKAKIQDKEGIPPDQQRLIFAGKQLEDGRTLSD*
NIQKESTLHLVLR LRGGMVSKGEELFTGVVPILVELDGDVNGHKFSVSGEGEGDATY GKL
LKFICTTGKLPVPWPTLVTTLT YGVQCFSRYPDHMKQHDFFKSAMPEGYVQERTIFFKDDG
NYKTRAEVKFEGDTLVNRIELKGIDFKEDGNILGHKLEYNYNSHNVYIMADKQKNGIKVNFKI
RHNIEDGGSVQLADHYQQNTPIGDGPVLLPDNHYLSTQSALS KDPNEKRDHMLLEFVTAAG
ITLGMDELYKRS HHHHHH

Ub-Y59TAG-cpsfGFP sequence (* denotes the UAA site):

MQIFVKLT LTKGTITLEVEPSDTIENVKAKIQDKEGIPPDQQRLIFAGKQLEDGRTLSD*
NIQKESTLHLVLR LRGGMGSSPYNSHKVYITADKQKNGIKVNFKIRHNVEDGGSVQLADHYQ
QNTPIGDGPVLLPDNHYLSTQSVLSKDPNEKRDHMLLEFVTAAGITLGMDELYKVDGGSG
GTGVSKGEELFTGVVPILVELDGDVNGHKFSVRGEGEGDATNGKLT LKFICTTGKLPVPWP
TLVTTLT YGVQCFSRYPDHMKQHDFFKSAMPEGYVQERTIFFKDDGTYKTRAEVKFEGDTL
VNRIELKGIDFKEDGNILGHKLEYNWRSHHHHHH

Ub-Y59TAG-sfGFP sequence (* denotes the UAA site):

MQIFVKLT LTKGTITLEVEPSDTIENVKAKIQDKEGIPPDQQRLIFAGKQLEDGRTLSD*
NIQKESTLHLVLR LRGGMVSKGEELFTGVVPILVELDGDVNGHKFSVRGEGEGDATNGKLT
LKFICTTGKLPVPWPTLVTTLT YGVQCFSRYPDHMKRHDFFKSAMPEGYVQERTISFKDDG
TYKTRAEVKFEGDTLVNRIELKGIDFKEDGNILGHKLEYNFNSHNVYITADKQKNGIKANFKI
RHNVEDGGSVQLADHYQQNTPIGDGPVLLPDNHYLSTQSVLSKDPNEKRDHMLLEFVTAA
GITHGMDELYKGS HHHHHH

Ub-Y59TAG-sfGFP-16-1 sequence (* denotes the UAA site):

MQIFVKLT LTKGTITLEVEPSDTIENVKAKIQDKEGIPPDQQRLIFAGKQLEDGRTLSD*
NIQKESTLHLVLR LRGGSGLR SAGPAGPGRSGMVSKGEELFTGVVPILVELDGDVNGHKF
SVRGE GEGDATNGKLT LKFICTTGKLPVPWPTLVTTLT YGVQCFSRYPDHMKRHDFFKSA
MPEGYVQERTISFKDDGTYKTRAEVKFEGDTLVNRIELKGIDFKEDGNILGHKLEYNFNSHN

VYITADKQKNGIKANFKIRHNVEDGSVQLADHYQQNTPIGDGPVLLPDNHYLSTQSVLSKDP
NEKRDHMLLEFVTAAGITHGMDELYKGSHHHHHH

Ub-Y59TAG-sfGFP-16-2 sequence (* denotes the UAA site):

MQIFVKTLTGKTITLEVEPSDTIENVKAKIQDKEGIPPDQQRLIFAGKQLEDGRTLSD*
NIQKESTLHLVLRLRGGIAWPLAGPAGPGGRSGMVSKGEELFTGVVPILVELDGDVNGHKF
SVRGE GEGDATNGKLT LKFICTTGKLPVPWPTLVTTLYGVQCFSRYPDHMKRHDFFKSA
MPEGYVQERTISFKDDGTYKTRAEVKFEGDTLVNRIELKGIDFKEDGNILGHKLEYNFNESHN
VYITADKQKNGIKANFKIRHNVEDGSVQLADHYQQNTPIGDGPVLLPDNHYLSTQSVLSKDP
NEKRDHMLLEFVTAAGITHGMDELYKGSHHHHHH

Ub-Y59TAG-sfGFP-21 sequence (* denotes the UAA site):

MQIFVKTLTGKTITLEVEPSDTIENVKAKIQDKEGIPPDQQRLIFAGKQLEDGRTLSD*
NIQKESTLHLVLRLRGGIAWPLSGLRSAGPAGPGGRSGMVSKGEELFTGVVPILVELDGDV
NGHKFSVRGE GEGDATNGKLT LKFICTTGKLPVPWPTLVTTLYGVQCFSRYPDHMKRHD
FFKSAMPEGYVQERTISFKDDGTYKTRAEVKFEGDTLVNRIELKGIDFKEDGNILGHKLEYN
FNESHNVYITADKQKNGIKANFKIRHNVEDGSVQLADHYQQNTPIGDGPVLLPDNHYLSTQS
VLSKDPNEKRDHMLLEFVTAAGITHGMDELYKGSHHHHHH

Ub-Y59TAG-Ub-sfGFP sequence (* denotes the UAA site):

MQIFVKTLTGKTITLEVEPSDTIENVKAKIQDKEGIPPDQQRLIFAGKQLEDGRTLSD*
NIQKESTLHLVLRLRGGMQIFVKTLTGKTITLEVEPSDTIENVKAKIQDKEGIPPDQQRLIFAG
KQLEDGRTLSDYNIQKESTLHLVLRLRAAMVSKGEELFTGVVPILVELDGDVNGHKFSVRG
EGEGDATNGKLT LKFICTTGKLPVPWPTLVTTLYGVQCFSRYPDHMKRHDFFKSAMPEG
YVQERTISFKDDGTYKTRAEVKFEGDTLVNRIELKGIDFKEDGNILGHKLEYNFNESHNVYITA
DKQKNGIKANFKIRHNVEDGSVQLADHYQQNTPIGDGPVLLPDNHYLSTQSVLSKDPNEKR
DHMLLEFVTAAGITHGMDELYKGSHHHHHH

Reference

1. Schauer, N. J.; Liu, X.; Magin, R. S.; Doherty, L. M.; Chan, W. C.; Ficarro, S. B.; Hu, W.; Roberts, R. M.; Iacob, R. E.; Stolte, B.; Giacomelli, A. O.; Perera, S.; McKay, K.; Boswell, S. A.; Weisberg, E. L.; Ray, A.; Chauhan, D.; Dhe-Paganon, S.; Anderson, K. C.; Griffin, J. D.; Li, J.; Hahn, W. C.; Sorger, P. K.; Engen, J. R.; Stegmaier, K.; Marto, J. A.; Buhrlage, S. J., Selective USP7 inhibition elicits cancer cell killing through a p53-dependent mechanism. *Sci. Rep.* **2020**, *10* (1), 5324.
2. Weinstock, J.; Wu, J.; Cao, P.; Kingsbury, W. D.; McDermott, J. L.; Kodrasov, M. P.; McKelvey, D. M.; Suresh Kumar, K. G.; Goldenberg, S. J.; Mattern, M. R.; Nicholson, B., Selective Dual Inhibitors of the Cancer-Related Deubiquitylating Proteases USP7 and USP47. *ACS Med. Chem. Lett.* **2012**, *3* (10), 789-792.
3. Altun, M.; Kramer, Holger B.; Willems, Lianne I.; McDermott, Jeffrey L.; Leach, Craig A.; Goldenberg, Seth J.; Kumar, K. G. S.; Konietzny, R.; Fischer, R.; Kogan, E.; Mackeen, Mukram M.; McGouran, J.; Khoronenkova, Svetlana V.; Parsons, Jason L.; Dianov, Grigory L.; Nicholson, B.; Kessler, Benedikt M., Activity-Based Chemical Proteomics Accelerates Inhibitor Development for Deubiquitylating Enzymes. *Chem. Biol.* **2011**, *18* (11), 1401-1412.
4. Turnbull, A. P.; Ioannidis, S.; Krajewski, W. W.; Pinto-Fernandez, A.; Heride, C.; Martin, A. C. L.; Tonkin, L. M.; Townsend, E. C.; Buker, S. M.; Lancia, D. R.; Caravella, J. A.; Toms, A. V.; Charlton, T. M.; Lahdenranta, J.; Wilker, E.; Follows, B. C.; Evans, N. J.; Stead, L.; Alli, C.; Zarayskiy, V. V.; Talbot, A. C.; Buckmelter, A. J.; Wang, M.; McKinnon, C. L.; Saab, F.; McGouran, J. F.; Century, H.; Gersch, M.; Pittman, M. S.; Marshall, C. G.; Raynham, T. M.; Simcox, M.; Stewart, L. M. D.; McLoughlin, S. B.; Escobedo, J. A.; Bair, K. W.; Dinsmore, C. J.; Hammonds, T. R.; Kim, S.; Urbé, S.; Clague, M. J.; Kessler, B. M.; Komander, D., Molecular basis of USP7 inhibition by selective small-molecule inhibitors. *Nature* **2017**, *550* (7677), 481-486.
5. Kategaya, L.; Di Lello, P.; Rougé, L.; Pastor, R.; Clark, K. R.; Drummond, J.; Kleinheinz, T.; Lin, E.; Upton, J.-P.; Prakash, S.; Heideker, J.; McClelland, M.; Ritorto, M. S.; Alessi, D. R.; Trost, M.; Bainbridge, T. W.; Kwok, M. C. M.; Ma, T. P.; Stiffler, Z.; Brasher, B.; Tang, Y.; Jaishankar, P.; Hearn, B. R.; Renslo, A. R.; Arkin, M. R.; Cohen, F.; Yu, K.; Peale, F.; Gnad, F.; Chang, M. T.; Klijjn, C.; Blackwood, E.; Martin, S. E.; Forrest, W. F.; Ernst, J. A.; Ndubaku, C.; Wang, X.; Beresini, M. H.; Tsui, V.; Schwerdtfeger, C.; Blake, R. A.; Murray, J.; Maurer, T.; Wertz, I. E., USP7 small-molecule inhibitors interfere with ubiquitin binding. *Nature* **2017**, *550* (7677), 534-538.
6. Summerer, D.; Chen, S.; Wu, N.; Deiters, A.; Chin, J. W.; Schultz, P. G., A genetically encoded fluorescent amino acid. *Proc. Natl. Acad. Sci. U.S.A.* **2006**, *103* (26), 9785-9789.
7. Wang, J.; Xie, J.; Schultz, P. G., A Genetically Encoded Fluorescent Amino Acid. *J. Am. Chem. Soc.* **2006**, *128* (27), 8738-8739.
8. Lee, H. S.; Guo, J.; Lemke, E. A.; Dimla, R. D.; Schultz, P. G., Genetic Incorporation of a Small, Environmentally Sensitive, Fluorescent Probe into Proteins in *Saccharomyces cerevisiae*. *J. Am. Chem. Soc.* **2009**, *131* (36), 12921-12923.
9. Chatterjee, A.; Guo, J.; Lee, H. S.; Schultz, P. G., A Genetically Encoded Fluorescent Probe in Mammalian Cells. *J. Am. Chem. Soc.* **2013**, *135* (34), 12540-12543.
10. Speight, L. C.; Muthusamy, A. K.; Goldberg, J. M.; Warner, J. B.; Wissner, R. F.; Willi, T. S.; Woodman, B. F.; Mehl, R. A.; Petersson, E. J., Efficient Synthesis and In Vivo Incorporation of Acridon-2-ylalanine, a Fluorescent Amino Acid for Lifetime and Förster

Resonance Energy Transfer/Luminescence Resonance Energy Transfer Studies. *J. Am. Chem. Soc.* **2013**, *135* (50), 18806-18814.

11. Jones, C. M.; Robkis, D. M.; Blizzard, R. J.; Munari, M.; Venkatesh, Y.; Mihaila, T. S.; Eddins, A. J.; Mehl, R. A.; Zagotta, W. N.; Gordon, S. E.; Petersson, E. J., Genetic encoding of a highly photostable, long lifetime fluorescent amino acid for imaging in mammalian cells. *Chem. Sci.* **2021**, *12* (36), 11955-11964.

12. Luo, J.; Uprety, R.; Naro, Y.; Chou, C.; Nguyen, D. P.; Chin, J. W.; Deiters, A., Genetically Encoded Optochemical Probes for Simultaneous Fluorescence Reporting and Light Activation of Protein Function with Two-Photon Excitation. *J. Am. Chem. Soc.* **2014**, *136* (44), 15551-15558.

13. Lampkowski, J. S.; Uthappa, D. M.; Young, D. D., Site-specific incorporation of a fluorescent terphenyl unnatural amino acid. *Bioorg. Med. Chem. Lett.* **2015**, *25* (22), 5277-5280.

14. Yamaguchi, Y.; Matsubara, Y.; Ochi, T.; Wakamiya, T.; Yoshida, Z.-i., How the π Conjugation Length Affects the Fluorescence Emission Efficiency. *J. Am. Chem. Soc.* **2008**, *130* (42), 13867-13869.

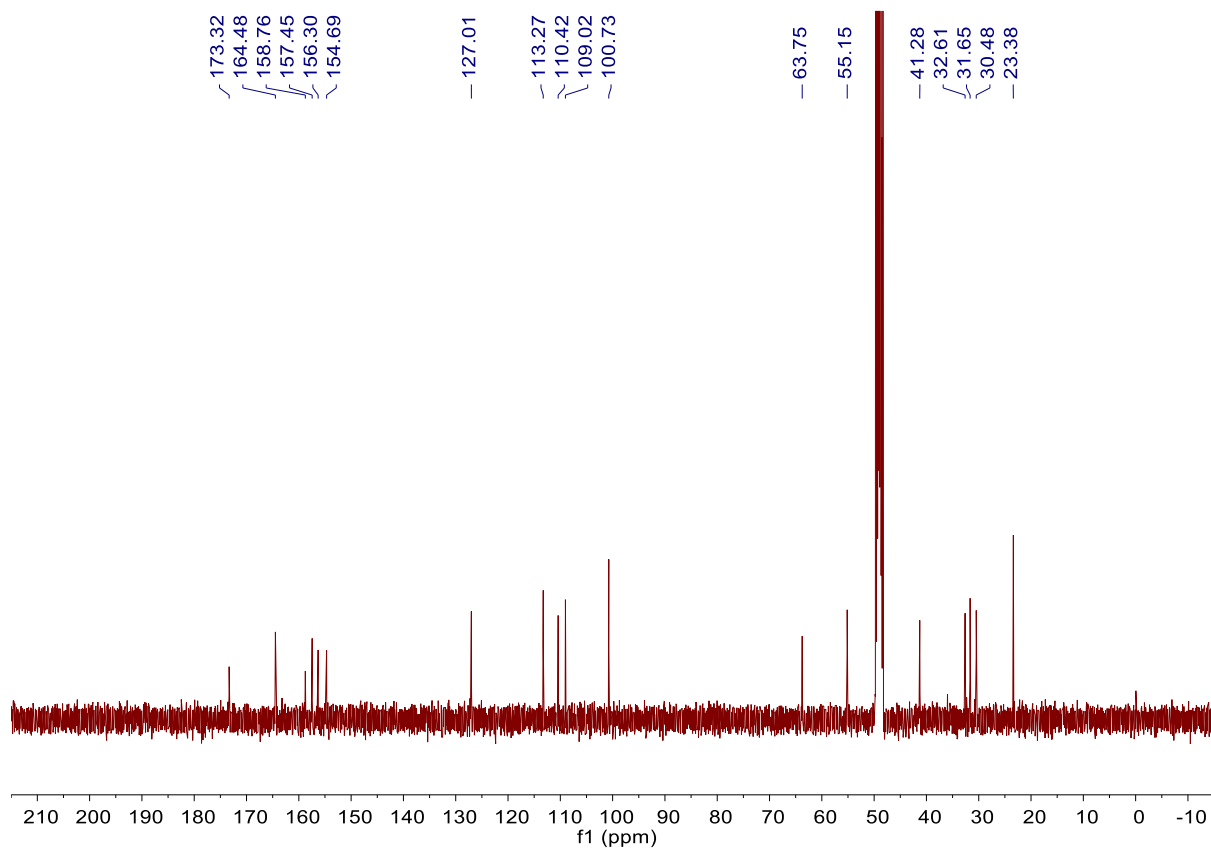
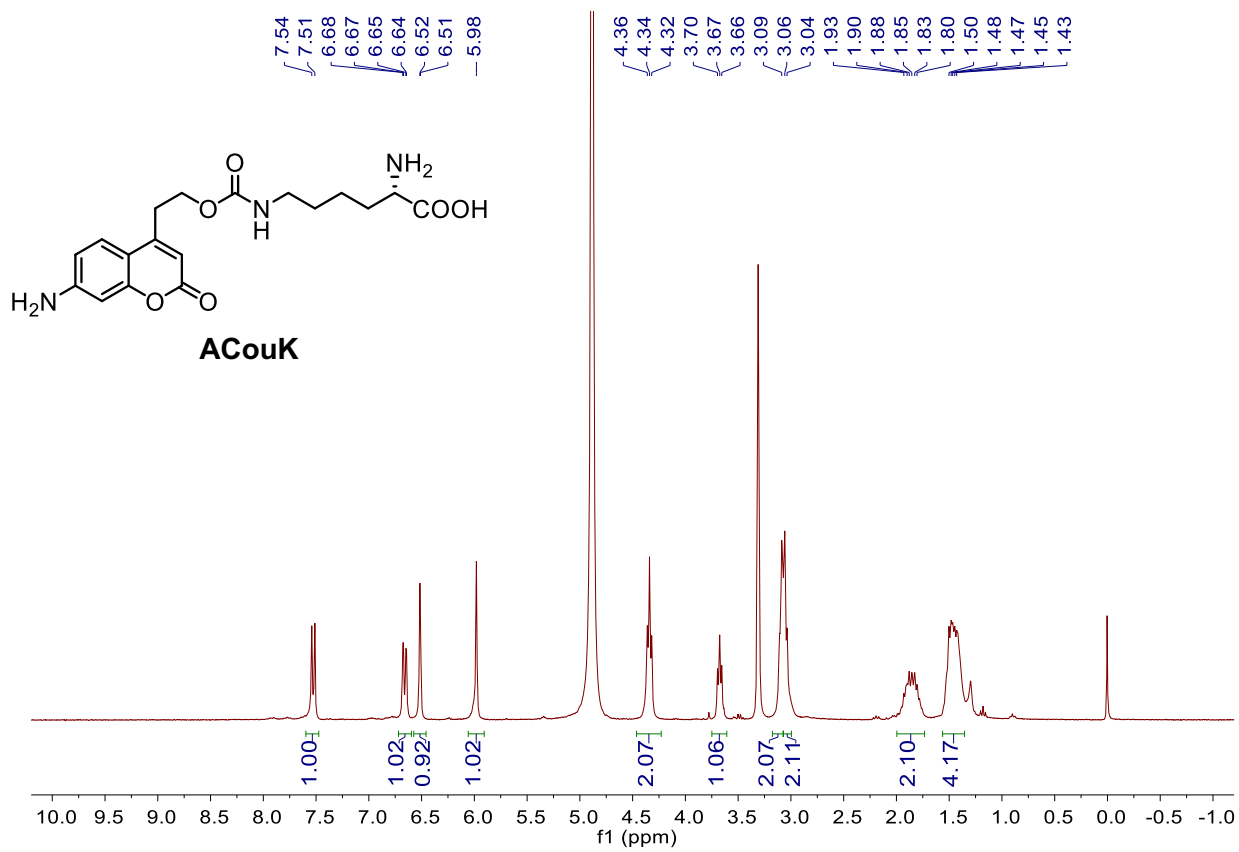
15. Wei, C.; Wang, R.; Wei, L.; Cheng, L.; Li, Z.; Xi, Z.; Yi, L., o-Fluorination of Aromatic Azides Yields Improved Azido-Based Fluorescent Probes for Hydrogen Sulfide: Synthesis, Spectra, and Bioimaging. *Chemistry – An Asian Journal* **2014**, *9* (12), 3586-3592.

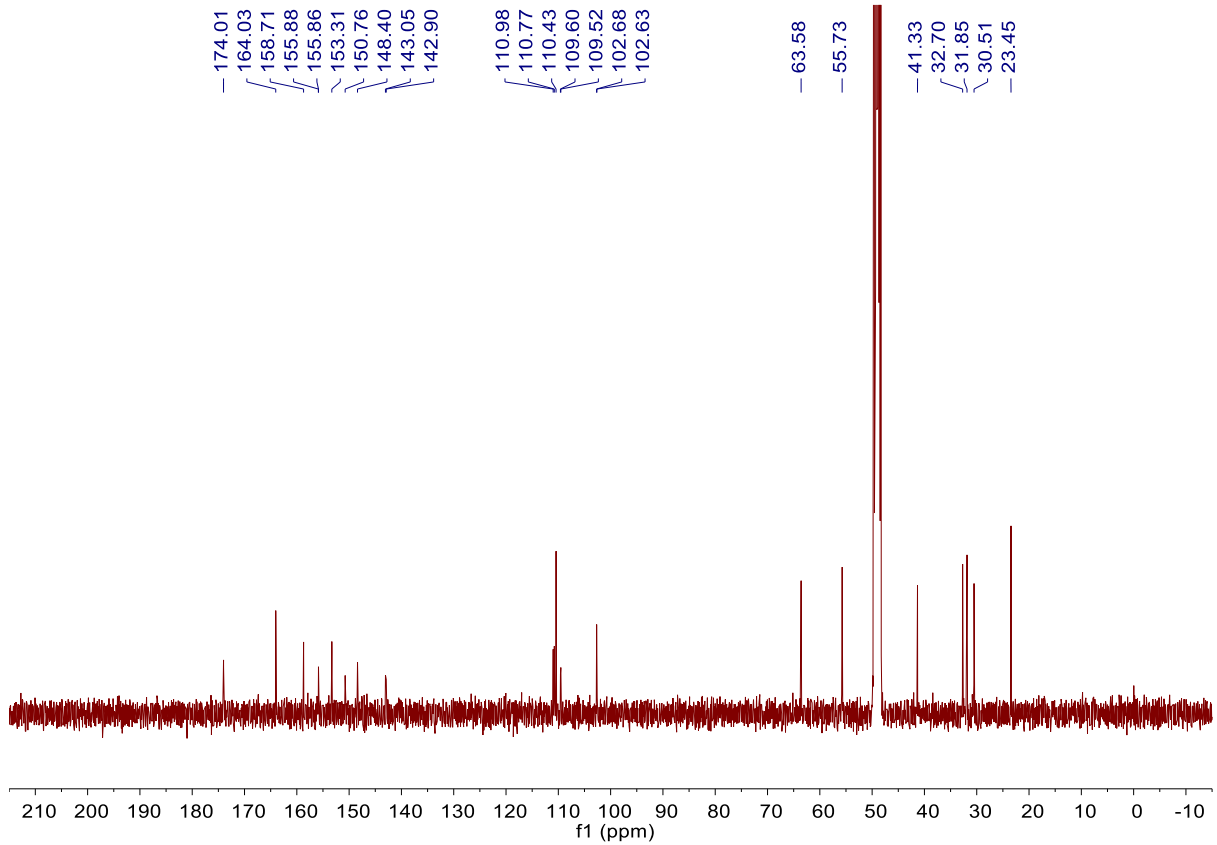
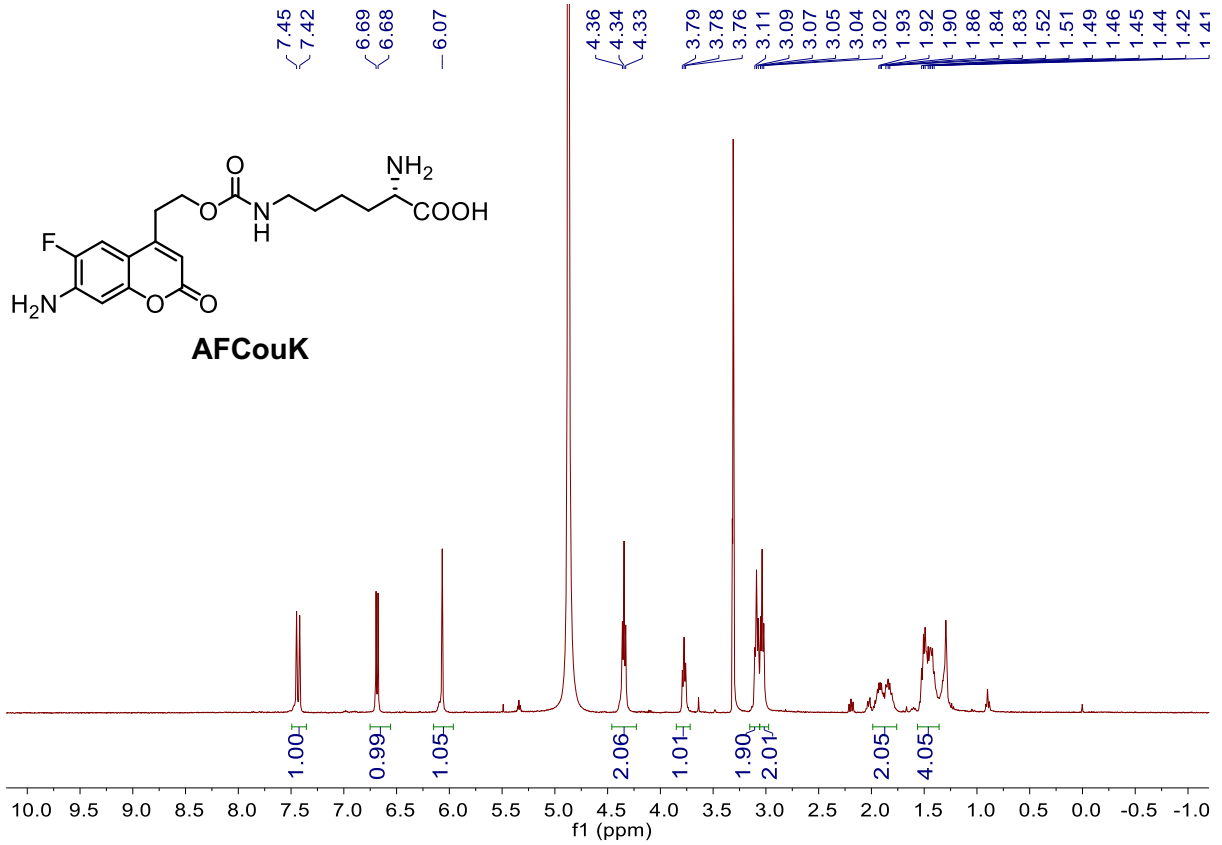
16. Zhang, Y.; Du, Y.; Li, M.; Zhang, D.; Xiang, Z.; Peng, T., Activity-Based Genetically Encoded Fluorescent and Luminescent Probes for Detecting Formaldehyde in Living Cells. *Angew. Chem. Int. Ed.* **2020**, *59* (38), 16352-16356.

17. Schmied, W. H.; Elsässer, S. J.; Uttamapinant, C.; Chin, J. W., Efficient Multisite Unnatural Amino Acid Incorporation in Mammalian Cells via Optimized Pyrrolysyl tRNA Synthetase/tRNA Expression and Engineered eRF1. *J. Am. Chem. Soc.* **2014**, *136* (44), 15577-15583.

18. Peng, T.; Hang, H. C., Site-Specific Bioorthogonal Labeling for Fluorescence Imaging of Intracellular Proteins in Living Cells. *J. Am. Chem. Soc.* **2016**, *138* (43), 14423-14433.

NMR spectra





Supplementary full gels and blots

Fig. 1D

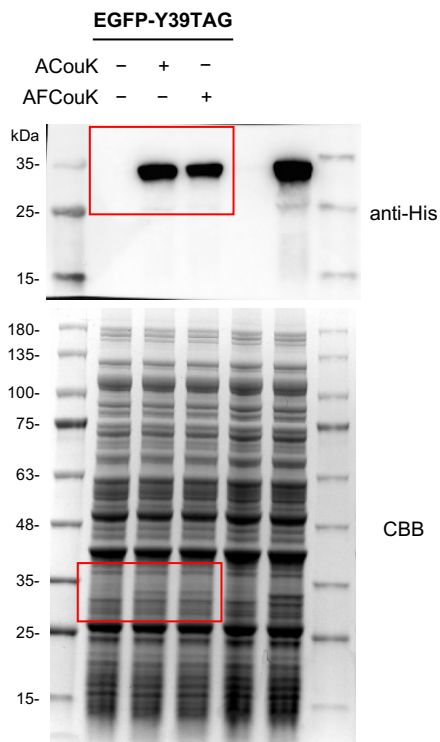


Fig. 1E

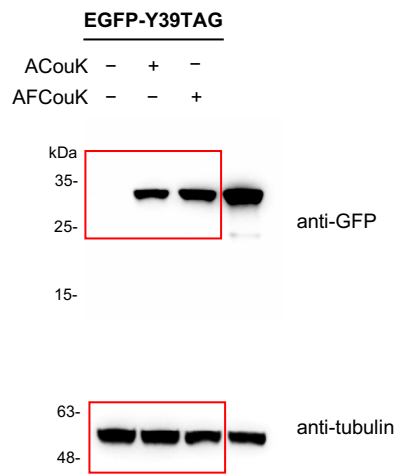
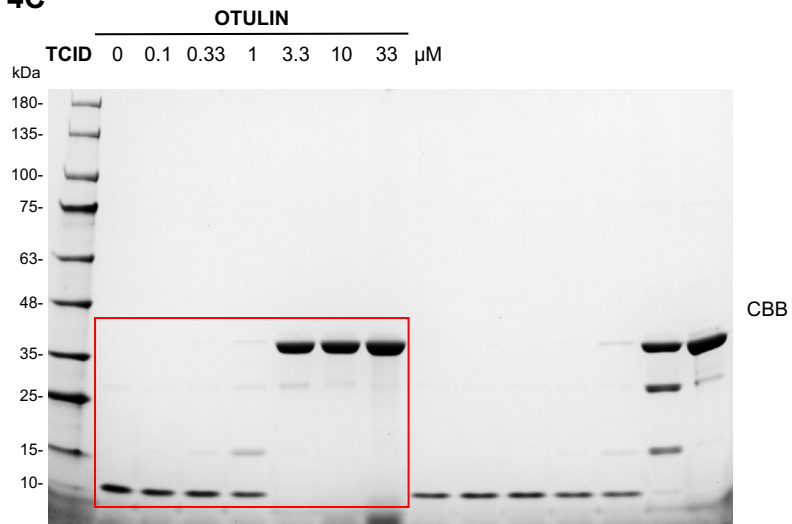


Fig. 4C



Full western blots and gels in the manuscript.

Fig. S4

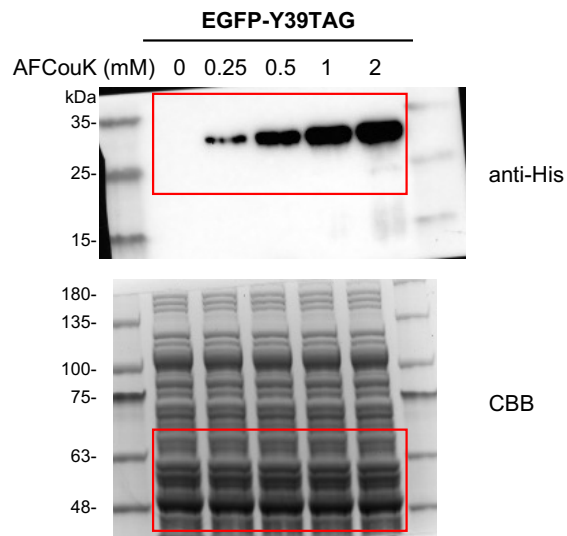


Fig. S19



Full western blots and gels in Fig. S4 and S19.